sciendo
Control and Cybernetics
vol. **53** (2024) No. 4
pages: 533-568
DOI: 10.2478/candc-2024-0022

An LMI based chaotic passivity analysis on memristive neural networks for memductance function*

by

R. Suvetha and P. Prakash†

Department of Mathematics, Periyar University, Salem, 636-011, India
†Corresponding author pprakashmaths@gmail.com
suvetharishi96@gmail.com

Abstract: This paper is devoted to passivity analysis for a class of chaotic memristive neural networks with distinct memductance approach, subject to actuator failures. Based on the existence of memristor, actuators and activation function, it was possible for the proposed model to stay in a stable state and reach the critical point by designing a strong reliable state-feedback controller. The qualitative analysis of this model can be developed using differential inclusion theory in the sense of Fillipov's solution with suitable Lyapunov functional to acquire the results in terms of linear matrix inequalities (LMIs). Considering the known and unknown actuators cases, some sufficient conditions are derived for both state-dependent switched system and state-dependent continuous system based on passivity theory along with its chaotic phenomena. The reliable state-feedback controller is designed to guarantee that the considered closed loop system is internally stable by adopting the stabilizing control law. Finally, numerical examples are presented to demonstrate theoretical results via graphical illustrations.

Keywords: passivity, memristive neural networks, actuator failure, linear matrix inequality, reliable controller

1. Introduction

Neural networks (NNs) have been extensively studied and successfully implemented in remarkable applications, due to the capability to simulate certain functions of human brain in many science and engineering domains. NNs technologies have risen to prominence because they can assist human intelligence with powerful processing. In the design of dynamical neural networks, the

*Submitted: March 2023; Accepted: May 2025.

steady state characteristics of NNs are quite important. In this context, but also for other essential reasons, interest developed in memristive neural networks (MNNs), a unique type of NNs, which have garnered a lot of attention recently (Pershin and Ventra, 2010; Xiao, Zhong and Li, 2015; Wang et al., 2018, 2020). Memristors are a type of state-dependent non-linear circuit components. In 1971, Chua predicted that a new significant two-terminal component called memristor will be used in electronic circuits inevitably (Chua, 1971), and the HP research team implemented it for the first time in 2008 (Strukov et al., 2008). MNNs are a revolutionary concept that is employed to comprehend the behavior of several physical, biological, and technical systems. One of the most promising applications of MNNs is associated with their potential to replicate the functioning of human brain.

Passivity theory is a key concept that originated from circuit analysis and system theory in 1970s and Bevelevich was the one to set forth it first (Bevelevich, 1968). It scrutinizes the internal stability of a model using input-output associated with features and can be used in a wide range of disciplines, such as complexity, signal processing, chaos control, and fuzzy control. The passive features keep the system internally stable. In Guo, Wang and Yan (2014), the authors explored the passivity and passification of a class of memristor based recurrent neural networks (RNNs) with time-varying delays, using the characteristic function technique. Finite-time passivity and synchronization criteria for coupled MNNs with and without delay have been studied in Huang, Qiu and Ren (2020). A delay–dependent Lagrange stability for memristor based uncertain neural networks (UNNs) with time-varying delay in terms of LMI technique have been proposed by Suresh, Syed Ali and Saroha (2023). For fuzzy fractional-order NNs with additive time-varying delays, a delay-dependent LMI-based passivity condition has been developed utilizing an indirect Lyapunov technique in Padmanaja and Balasubramanian (2022). Based on the Lyapunov functional approach, a new passivity criterion for fractional-order NNs was discussed in Shafiya and Nagamani (2022). By employing inequality techniques and Lyapunov function theories, finite-time stabilization of NNs was developed based on finite-time passivity theory, in Xiao and Zheng (2020). A new delay dependent passivity criterion for UNNs was formulated by Song and Wang (2010) with the use of the LMI technique. Based on free-matrix integral inequality and improved Lyapunov-Krasovskii functional (LKF), the robust passivity analysis for a class of blue UNNs with discrete and distributed time-varying delays has been addressed in Park, Hua and Shi (2019). This context of respective research is the first motivation of the present research.

Despite the fact that only specific research findings on memductance function are now available, they are productive till now (Wu and Zheng, 2014; Anbuvithya et. al., 2016; Liu and Xu, 2016). In 2014, a state-dependent switched and continuous memductance function based passivity analysis for MNNs was published by Wu and Zheng (2014). The passivity criterion for BAMNNs (Bideidectional Associative Memory Neural Networks) with memductance function has been examined in Anbuvithya et al. (2016) utilizing correct LKF construction and differential inclusions theory. A class of MNNs with mixed time-varying delays was studied in Liu and Xu (2016) for state-dependent memductance function. A μ-stability analysis of memristor based RNNs with different memductance approach, which is characterized by two distinct systems: the state dependent switched system and the state dependent continuous system, was considered in Chandrasekar, Rakkiyappan and Li (2016) with effects of leakage delay. Recently, an event-triggered synchronization problem of delayed stochastic NNs was investigated in terms of LMI technique in Vadivel et al. (2023). By using the Razumikhin fractional-order theorem, an improved delay-dependent passivity criteria for fractional-order NNs with bounded time-varying delay was demonstrated in Sau, Thuan and Huyen (2020). This is the second motivation of the present research.

On the other hand, time delay is an unavoidable phenomenon that emerges in most physical circuits and makes the respective system perform in an unstable manner. It is crucial to investigate the time-delay systems, since delays are a primary factor in system instability, divergence, and oscillation. If there is a significant delay between system's input and output, the system may become unstable and function worse than optimally. The fractional-order passivity and passification of MNNs with time-delay have been analyzed and solved using differential inclusion theory, set valued maps, and the LMI technique in Ding et al. (2013). By employing a new summation inequality technique, passivity analysis for a class of discrete-time linear systems was studied in Qiu et al. (2019). A new passivity criterion for UNNs with time-varying delay was addressed in Li et al. (2016). Reciprocal convex approach was proposed in Zheng, Park and Shen (2015) for effective passivity analysis with discrete and distributed delay. Passivity analysis of UNNs with discrete and distributed delay, based on convex approach has been performed in Yang et al. (2018). This is the third motivation of the present study.

For the past few years, reliable state-feedback control has received a lot of attention, since unanticipated failures could cause significant harm and possibly pose a risk to the environment, see Junfeng, Li and Raissi (2020). In Yang, Cocquempot and Jiang (2008), authors introduced the passivity analysis into fault tolerance analysis for switched systems. In accordance with the feedback control strategy and LMI technique, the passivity of multiple weighted coupled MNNs guarantees passive, output strictly passive, and input strictly passive behavior, as detailed in Wang et al. (2022). Robust passivity and feedback passification of a class of uncertain fractional-order linear systems were demonstrated using matrix singular value decomposition and LMI techniques in Chen et al. (2019).

Failures of the actuators in control systems can seriously impair their performance, see Gu et al. (2020). During the occurrence of actuator, sensor or other component errors, a fault-tolerant control has the capacity to self-correct system behavior. Besides, faults might occur due to uncertain parameters, mechanical exhaustion and external disturbances in actuators. It is very important to overcome all these consequences in the model to reduce the fault occurrence, see Zhang, Li and Raissi (2020). Many researchers are interested in incorporating switching processes into characterizing sudden alterations of dynamic systems due to abrupt changes in systems. This is the fourth motivation of the study here reported.

Motivated by the above outlined issues, the main aim of this work is to perform the passivity analysis of MNNs model with switched and continuous function of uncertain time-varying delay with the help of set-valued map, differential inclusion theory, reliable state feedback controller and accounting for actuator faults, so as to guarantee the fulfilment of internal stability criteria. The concept of passivity has been extensively studied in previous investigations (Anbuvithya et al., 2016, Ding et al., 2023, Li et al., 2016). The present study offers several innovative and significant contributions. The major contributions of this study are the following ones:

1. This study fills the gap concerning the framework of chaotic passivity analysis of MNNs model for state-dependent switched system and state-dependent continuous system with the effects of actuator failure cases.
2. In accordance with the memductance function, both known and unknown cases were taken into account subject to actuator failures by designing reliable state-feedback controller for the MNN model.
3. By utilizing Lyapunov stability theory, differential inclusion theory, and set valued mappings, a novel set of sufficient conditions has been formulated that ensures the internal state stability via the LMI framework. These conditions are established under the well-defined hypotheses that satisfy the activation function properties, through the design of an appropriate controller gain matrix.
4. A strong fault-tolerant control law is implemented to derive the main results with Definition 1, related to passivity, by implementing Wirtinger's integral inequality, Jensen's inequality, schur complement and congruence transformation. In contrast to Anbuvithya et al. (2016), Liu et al. (2016), Wu and Zeng (2014), the memductance function's chaotic behaviour for the passive model has been specified.
5. Finally, simulation examples have been produced and analyzed by an effective LMI control toolbox via MATLAB for feasible outcomes in generic and chaotic forms.

This paper is organized as follows: In Section 2, the problem of MNNs is modeled and some necessary lemmas and inequalities are provided. In Section 3, the main results are derived for state-dependent switched MNNs and state-dependent continuous MNNs for passivity criteria. In Section 4, the numerical simulations are given, meant to verify the effectivenes of results.

2. Problem formulation and preliminaries

Based on the physical characteristics of the memristor, the general class of MNNs is constructed for an i^{th} subsystem as follows:

$$\begin{aligned}\dot{\upsilon}_i(\theta) &= -\Gamma_i(\upsilon_i(\theta))\upsilon_i(\theta) + \sum_{j=1}^{n} e_{ij}(\upsilon_i(\theta))\tilde{g}_j(\upsilon_j(\theta)) \\ &\quad + \sum_{j=1}^{n} h_{ij}(\upsilon_i(\theta))\tilde{g}_j(\upsilon_j(\theta - d(\theta))) + u_i(\theta),\end{aligned} \tag{1}$$

where $\Gamma_i(\upsilon_i(\theta)) = \frac{1}{C_i}\Big[\sum_{j=1}^{n}(\check{M}_{ij} + \check{W}_{ij}) \times \delta_{ij} + \bar{R}_i\Big]$, $e_{ij}(\upsilon_i(\theta)) = \frac{\check{M}_{ij}}{C_i} \times \delta_{ij}$, and $h_{ij}(\upsilon_i(\theta - d(\theta))) = \frac{\check{W}_{ij}}{C_i} \times \delta_{ij}$, $i = 1, 2, \cdots, n$. In this formulation, $\delta_{ij} = 1$, if $i \neq j$ holds, otherwise, $\delta_{ij} = -1$ if $i = j$. $\check{M}_{ij}$ and $\check{W}_{ij}$ denote the memductances of memristors $\mathcal{R}^{*}_{ij}$ and $\mathcal{R}^{**}_{ij}$, respectively. $\mathcal{R}^{*}_{ij}$ represents the memristor that relates the neuron activation function $\tilde{g}_j(\upsilon_j(\theta))$ and $\upsilon_i(\theta)$; $\mathcal{R}^{**}_{ij}$ denotes the memristor facilitating the interaction between the neuron activation function $\tilde{g}_j(\upsilon_j(\theta - d(\theta)))$ and $\upsilon_i(\theta)$. Then, $\bar{R} = \frac{1}{R^*}$, where R^* represents the parallel resistor, corresponding to the capacitor C_i. Γ_i denotes the self-feedback connection weights of i-th neuron cell; $\upsilon_i(\theta)$ denotes the state variable; $e_{ij}(\upsilon_i(\theta))$ and $h_{ij}(\upsilon_i(\theta))$ denotes the memristive connection weights; $\tilde{g}_j(\upsilon_j(\theta))$ symbolizes the activation function, which is continuous in general; $\tilde{g}_j(\upsilon_j(\theta - d(\theta)))$ stands for continuous feedback activation function, where the activation functions are both differentiable and bounded; θ symbolizes time; $u_i(\theta)$ denotes the continuous control process on the ith unit; $d(\theta)$ is time-varying delay, where $d \geq 0$ is known to be the upper delay bound.

Along with the features of the memristor, the connection weights considered in the system (1), will be of the form,

$$e_{ij}(\upsilon_i(\theta)) = \begin{cases} \hat{e}_{ij}, & |\upsilon_i(\theta)| \leq \eta_i, \\ \check{e}_{ij}, & |\upsilon_i(\theta)| > \eta_i, \end{cases} \quad h_{ij}(\upsilon_i(\theta)) = \begin{cases} \hat{h}_{ij}, & |\upsilon_i(\theta)| \leq \eta_i, \\ \check{h}_{ij}, & |\upsilon_i(\theta)| > \eta_i, \end{cases}$$

where the switching jumps $\eta_i > 0$ are non-negative and $\hat{e}_{ij}$, $\check{e}_{ij}$, $\hat{h}_{ij}$ and $\check{h}_{ij}$ are constants.

According to recent studies, memristive device fingerprints can be handled by pinched hysteresis loops. The pinched hysteresis loop is caused by the material's restricted capacity to respond to increase in the magnetic field once it reaches saturation. The proclivity or process of evolution of memristive systems takes several forms under various pinched hysteresis loops. The non-linearity of the memductance function is widely acknowledged as the cause of the pinched hysteresis loop. According to the physical structure of memristors, we have

$$\check{W}_{ij} = \frac{dq_{ij}}{d\mu_{ij}}; \quad \check{M}_{ij} = \frac{d\bar{q}_{ij}}{d\bar{\mu}_{ij}};$$

where q_{ij} and $\bar{q}_{ij}$ denote charge, while μ and $\bar{\mu}$ denote the magnetic flux corresponding to the memristors $\check{W}_{ij}$ and $\check{M}_{ij}$.

In this paper, we thoroughly examine both distinctive memductance functions, considering state-dependent switched as well as continuous cases, under the framework of a reliable state-feedback control strategy. We explore two alternative memductance function conditions based on the non-linear relationship between the current and the magnetic flux.

Case 1: The memductance tasks are given for the state-dependent switched system as

$$\check{W}_{ij} = \begin{cases} e_{ij}, & |\mu_{ij}| < l_{ij}, \\ h_{ij}, & |\mu_{ij}| > l_{ij}, \end{cases} \quad \text{and} \quad \check{M}_{ij} = \begin{cases} \acute{e}_{ij}, & |\bar{\mu}_{ij}| < \bar{l}_{ij}, \\ \acute{h}_{ij}, & |\bar{\mu}_{ij}| > \bar{l}_{ij}, \end{cases}$$

where e_{ij}, h_{ij}, $\acute{e}_{ij}$, $\acute{h}_{ij}$, l_{ij} and $\bar{l}_{ij}$ are constants. Further, μ_{ij} and $\bar{\mu}_{ij}$ denote the magnetic fluxes, corresponding to the memristors, whose memductances are $\check{W}_{ij}$ and $\check{M}_{ij}$, respectively.

Case 2: The memductance role for state-dependent continuous system is given by

$$\check{W}_{ij} = a_{ij} + 3b_{ij}\mu_{ij}^2 \quad \text{and} \quad \check{M}_{ij} = \tilde{a}_{ij} + 3\tilde{b}_{ij}\bar{\mu}_{ij}^2$$

where a_{ij}, b_{ij}, $\tilde{a}_{ij}$ and $\tilde{b}_{ij}$ are constants.

The unique characteristics of memristor and the current-voltage quality aspect arises according to the following two cases:

Case 1a: Consider the switched memductance function, where $e_{ij}(\upsilon_i(\theta))$ and $h_{ij}(\upsilon_i(\theta))$ are switching jumps, as considered in Case 1,

$$e_{ij}(\upsilon_i(\theta)) = \begin{cases} \hat{e}_{ij}, & |\upsilon_i(\theta)| \leq \eta_i, \\ \check{e}_{ij}, & |\upsilon_i(\theta)| > \eta_i, \end{cases} \quad \text{and} \quad h_{ij}(\upsilon_i(\theta)) = \begin{cases} \hat{h}_{ij}, & |\upsilon_i(\theta)| \leq \eta_i, \\ \check{h}_{ij}, & |\upsilon_i(\theta)| > \eta_i, \end{cases}$$

where the switching jumps $\eta_i > 0$ are non-negative. Then, $\hat{e}_{ij}$, $\check{e}_{ij}$, $\hat{h}_{ij}$ and $\check{h}_{ij}$ are known constants. Based on the information provided in the above Case 1, $e_{ij}(\upsilon_i(\theta))$ and $h_{ij}(\upsilon_i(\theta))$ in this system have been classified according to the states $\upsilon_i(\theta)$ and $\upsilon_i(\theta - d(\theta))$. Evidently, the weights $e_{ij}(\upsilon_i)$ and $h_{ij}(\upsilon_i)$ are discontinuous (or) piece-wise continuous functions, with at most two points of discontinuity at η_i.

Case 2a: Consider the continuous memductance function from Case 2, where $e_{ij}(\upsilon_i(\theta))$ and $h_{ij}(\upsilon_i(\theta))$ are continuous functions

$$\underline{\Xi}_{ij} \le e_{ij} \le \overline{\Xi}_{ij}, \quad \underline{\Upsilon}_{ij} \le h_{ij} \le \overline{\Upsilon}_{ij},$$

in which the jumps $\underline{\Xi}_{ji}$, $\overline{\Xi}_{ij}$, $\underline{\Upsilon}_{ij}$ and $\overline{\Upsilon}_{ij}$ are constants.

By employing the definitions of set valued maps and the concept of differential inclusion for system (1), and taking into account the switching conditions specified for **Case 1a**,

$$\begin{aligned} \dot{\upsilon}_i(\theta) \in -\Gamma_i \upsilon_i(\theta) &+ \sum_{j=1}^{n} \tilde{co}[e_{ij}(\upsilon_i(\theta))]\, \tilde{g}_j(\upsilon_j(\theta)) \\ &+ \sum_{j=1}^{n} \tilde{co}[h_{ij}(\upsilon_i(\theta))]\, \tilde{g}_j(\upsilon_j(\theta - d(\theta))) + u_i(\theta), \end{aligned} \tag{2}$$

where $\tilde{co}[\mathbb{E}]$ symbolizes the convex hull of the given set $\mathbb{E}$,

$$\tilde{co}[e_{ij}(\upsilon_i(\theta))] = \begin{cases} \hat{e}_{ij}, & |\upsilon_i(\theta)| < \eta_i, \\ [\underline{e}_{ij}, \overline{e}_{ij}], & |\upsilon_i(\theta)| = \eta_i, \\ \check{e}_{ij}, & |\upsilon_i(\theta)| > \eta_i, \end{cases}$$

$$\tilde{co}[h_{ij}(\upsilon_i(\theta))] = \begin{cases} \hat{h}_{ij}, & |\upsilon_i(\theta)| < \eta_i, \\ [\underline{h}_{ij}, \overline{h}_{ij}], & |\upsilon_i(\theta)| = \eta_i, \\ \check{h}_{ij}, & |\upsilon_i(\theta)| > \eta_i, \end{cases}$$

and $\underline{e}_{ij} = min\{\hat{e}_{ij},\ \check{e}_{ij}\}$, $\overline{e}_{ij} = max\{\hat{e}_{ij},\ \check{e}_{ij}\}$, $\underline{h}_{ij} = min\{\hat{h}_{ij},\ \check{h}_{ij}\}$, $\overline{h}_{ij} = max\{\hat{h}_{ij}, \check{h}_{ij}\}$ for $i = 1, 2, \cdots, n$. At the same time, $\tilde{co}\big[e_{ij}(\upsilon_i)\big]$ (or $\tilde{co}\big[h_{ij}(\upsilon_i)\big]$) are intervals with non-empty interior when $e_{ij}(\upsilon_i)$ (or $h_{ij}(\upsilon_i)$) are piece-wise or discontinuous functions at $|\upsilon_i| = \eta_i$, respectively. Moreover, $\tilde{co}\big[e_{ij}(\upsilon_i)\big] = \{e_{ij}(\upsilon_i)\}$ (or $\tilde{co}\big[h_{ij}(\upsilon_i)\big] = \{h_{ij}(\upsilon_i)\}$) are singleton sets, when $e_{ji}(\upsilon_i)$ (or $h_{ij}(\upsilon_i)$) are continuous at υ_i, respectively.

Based on Case 1a, there exist $e_{ij}(\theta) \in \tilde{co}[e_{ij}(\upsilon_i(\theta))]$ and $h_{ij}(\theta) \in \tilde{co}[h_{ij}(\upsilon_i(\theta))]$ such that

$$\dot{\upsilon}(\theta) = -\Gamma \upsilon(\theta) + E(\theta)\, \tilde{g}(\upsilon(\theta)) + H(\theta)\, \tilde{g}(\upsilon(\theta - d(\theta))) + u(\theta), \tag{3}$$

where $E(\theta) = (E_{ij}(\theta))_{n\times n}$, $H(\theta) = (H_{ij}(\theta))_{n\times n}$, $\Gamma = diag\{\Gamma_1, \Gamma_2, \ldots, \Gamma_n\}$, $\upsilon(\theta) = \big[\upsilon_1(\theta), \upsilon_2(\theta), \ldots, \upsilon_n(\theta)\big]^T$, $\tilde{g}(\upsilon(\theta)) = \big[\tilde{g}(\upsilon_1(\theta)), \tilde{g}(\upsilon_2(\theta)), \ldots, \tilde{g}(\upsilon_n(\theta))\big]^T$

and $\tilde{g}(\upsilon(\theta-d(\theta))) = \left[\tilde{g}(\upsilon_1(\theta-d(\theta))), \tilde{g}(\upsilon_2(\theta-d(\theta))), \ldots, \tilde{g}(\upsilon_n(\theta-d(\theta)))\right]^T$, respectively.

Remark 1 *In most of the research studies, a memristor contains a basic junction that can change from a low resistance to a high resistance state, Zhang, Hu and Shen (2015). The alteration in pinched hysteresis loops arises due to changes in the memductance parameters $\check{W}_{ij}$ and $\check{M}_{ij}$ of the memristor. As a consequence, pinched hysteresis loops, which serve as the memristors unique fingerprints are the outcome, and they ensure the configuration of non-linear connectivity between voltage and current.*

Remark 2 *Passivity offers an excessively abstract metric of stability, based solely on how much energy a system uses. Consuming the input energy without producing any dissipated energy is another aspect of passivity (see Anbuvithya et al., 2016; Qiu et al., 2019). Systems that lack memory or self-sustaining activity are referred to as passive networks. Instead, they only react in response to the input they are provided at the moment. In order to ensure closed loop stability, the passivity shortfall of one system can be offset by the surplus passivity of another system, such as a controller.*

The main objective of the study here reported is to design the appropriate controller (i.e. the reliable one), which, in general, tolerates the failures. Here, we construct a fault model

$$\hat{u}_i(\theta) \quad = \quad r_i u_i(\theta), \tag{4}$$

where $u(\theta)$ is control input and r_i, $i = 1, 2, \ldots, n$, which indicates the permissible shortage and we denote $R = diag\{r_1, r_2, \ldots, r_n\}$, which is defined as

$$0 < \underline{R} = \mathrm{diag}\{\underline{r}_1, \ldots, \underline{r}_n\} \leq R = \mathrm{diag}\{r_1, \ldots, r_n\} \leq \overline{R} = \mathrm{diag}\{\overline{r}_1, \ldots, \overline{r}_n\} < I, \tag{5}$$

and $\hat{R} = diag\{\hat{r}_1, \ldots, \hat{r}_n\} = \frac{\underline{R}+\overline{R}}{2}$, $\check{R} = diag\{\check{r}_1, \ldots, \check{r}_n\} = \frac{\overline{R}-\underline{R}}{2}$,
hence, R can be rewritten as

$$R \quad = \quad \hat{R} + \Theta, \tag{6}$$

where $\Theta = \hat{R} + diag\{\zeta_1, \zeta_2, \ldots, \zeta_n\}$, $|\zeta_i| \leq \check{r}_i$. Moreover, the state-feedback stabilizing control law is defined by $u(\theta) = K\upsilon(\theta)$, where K stands for state-feedback gain matrix. At the same time, from (4), we acquire

$$\hat{u}(\theta) = \quad Ru(\theta) = RK\upsilon(\theta). \tag{7}$$

Now, $u(\theta)$ can be replaced with $\hat{u}(\theta)$, so that the control signal model will get restored as follows

$$\dot{\upsilon}(\theta) = -\Gamma\upsilon(\theta) + E(\theta)\,\tilde{g}(\upsilon(\theta)) + H(\theta)\,\tilde{g}(\upsilon(\theta-d(\theta))) + \hat{u}(\theta). \tag{8}$$

Hypotheses

(H1) The disseminating time-varying delay $d(\theta)$ and the uncertain element in time-varying delay $|\Delta_d(\theta)|$, which satisfies the condition $|\Delta_d(\theta)| \leq \delta_d$, where δ_d is a constant [?the sentence is incomplete?]. The non-negative continuous variable $d(\theta)$ can be represented as $0 \leq d(\theta) = d + \delta_d(\theta)$ and $d(\theta)$ is assumed to be differentiable and to satisfy $\dot{d}(\theta) \leq \sigma$, where σ stands for a positive constant.

(H2) For any $i = 1, 2, \ldots, n$, the activation functions $\tilde{g}_i$ are continuous functions for all υ_1, $\upsilon_2 \in \mathbb{R}$, and there exist constants J_i^- and J_i^+ such that

$$J_i^- \leq \frac{\tilde{g}_i(\upsilon_1) - \tilde{g}_i(\upsilon_2)}{\upsilon_1 - \upsilon_2} \leq J_i^+,\ \upsilon_1 \neq \upsilon_2. \tag{9}$$

For the sake of computational convenience, we make use of the following notations throughout this study.

$$R_1 = diag\{R_1^- \, R_1^+, R_2^- \, R_2^+, \ldots, R_n^- \, R_n^+\},$$

$$R_2 = diag\left\{\frac{R_1^- + R_1^+}{2}, \frac{R_2^- + R_2^+}{2}, \ldots, \frac{R_n^- + R_n^+}{2}\right\}.$$

Preliminaries

Now, we present some useful definition and lemmas, which are needed to derive our main results

Definition 1 (Rajchakit and Sriraman, 2021) *MNNs* (1) *is called passive if there exists a scalar $\lambda \leq 0$ such that*

$$2\int_0^{\theta_\upsilon} \tilde{g}^T(\upsilon(s))u(s)ds \geq -\lambda \int_0^{\theta_\upsilon} u^T(s)u(s)ds,$$

for all $\theta_\upsilon \geq 0$ and for all solutions of (3) *with $\upsilon(0) = 0$.*

Lemma 1 (Suresh and Manivannan, 2012) *For any constant matrix $T > 0$, the following inequality holds for all continuously differentiable functions $\nu(s)$: $[c, d] \to \mathbb{R}^n$*

$$(d-c)\int_c^d \nu^T(s)\, T\, \nu(s)ds \geq \left(\int_c^d \nu^T(s)ds\right) T \left(\int_c^d \nu(s)ds\right) + 3\varphi^T T\varphi,$$

where $\varphi = \int_c^d \nu(s)ds - \frac{2}{d-c}\int_c^d \int_c^s \nu(u)\, du\, ds$.

Lemma 2 (Wirtinger's inequality, Rajavel et al., 2018) *For given symmetric positive definite matrices $T > 0$ and for any differentiable signal $\Phi(s)$: $[c,d] \to \mathbb{R}^n$, the following inequality holds*

$$\int_c^d \dot{\upsilon}^T(s) T \dot{\upsilon}(s) ds \geq \frac{1}{d-c} \begin{bmatrix} \Phi(d) \\ \Phi(c) \\ \vartheta \end{bmatrix}^T W_2(T) \begin{bmatrix} \Phi(d) \\ \Phi(c) \\ \vartheta \end{bmatrix},$$

where $\vartheta = \dfrac{1}{d-c} \displaystyle\int_c^d \upsilon(s) ds,$

$$W_2(T) = W_0(T) + \tfrac{\pi^2}{4} \begin{bmatrix} T & T & -2T \\ * & T & -2T \\ * & * & 4T \end{bmatrix} \text{ and } W_0(T) = \begin{bmatrix} T & -T & 0 \\ * & T & 0 \\ 0 & 0 & 0 \end{bmatrix}.$$

Lemma 3 (Jensen's inequality, Zhang et al., 2021) *For matrix $T \in \mathbb{R}^{n \times n}$, $T = T^T > 0$, scalars $c < d$, vector $\nu(s) : [c,d] \to \mathbb{R}^n$ such that the integration concerned is well defined, there is*

$$(i)(d-c) \textstyle\int_c^d \nu^T(s) T \nu(s) ds \geq \left(\int_c^d \nu(s) ds \right)^T T \left(\int_c^d \nu(s) ds \right),$$

$$(ii) \tfrac{(d-c)^2}{2} \textstyle\int_c^d \int_{\theta+u}^{\theta} \nu^T(s) T \nu(s) ds\, du \geq \left(\int_c^d \int_{\theta+u}^{\theta} \nu(s) ds\, du \right)^T T \left(\int_c^d \int_{\theta+u}^{\theta} \nu(s) ds\, du \right).$$

Lemma 4 (Boyd et al., 1994) *Let Γ_1, Γ_2, Γ_3 be constant matrices, where $\Gamma_1 = \Gamma_1^T > 0$, $\Gamma_2 = \Gamma_2^T > 0$, then $\Gamma_1 + \Gamma_3 \Gamma_2^{-1} \Gamma_3 < 0$, if and only if* $\begin{bmatrix} \Gamma_1 & \Gamma_3^T \\ \Gamma_3 & -\Gamma_2 \end{bmatrix} < 0$.

3. Main results

In this section, a set of sufficient conditions is presented, based on constructing a suitable LKF along with the LMI technique for the model (1), which has non-smooth dynamics in nature. More precisely, we performed passivity analysis for state-dependent switched MNNs with reliable state-feedback controller. Further, we extended the original passivity analysis onto the state-dependent continuous MNNs.

3.1. State-dependent switched MNNs

In the following theorem, we address the switching law of MNNs with the objective of guaranteeing the fulfilment of passivity criteria for switched systems via a reliable controller, when actuator faults are known.

THEOREM 1 *Under hypothesis (H2) and for given scalars d and σ, the MNNs system (3) is passive in the presence of known actuator fault R, if there exist positive definite matrices $\bar{B} > 0$, $\bar{V} > 0$, $\bar{Q}_1 > 0$, $\bar{Q}_2 > 0$, $\bar{M} > 0$, $\bar{N} > 0$ and $\bar{Z} > 0$, diagonal matrices $\bar{G}_1 > 0$, $\bar{G}_2 > 0$, real matrices S, Y, with appropriate dimensions, and then the following LMIs holds:*

$$\tilde{\zeta} = \begin{bmatrix} \tilde{\zeta}_{1,1} & 0 & \tilde{\zeta}_{1,3} & \tilde{\zeta}_{1,4} & \tilde{\zeta}_{1,5} & 0 & \tilde{\zeta}_{1,7} & 0 & 0 \\ * & \tilde{\zeta}_{2,2} & 0 & 0 & 0 & 0 & 0 & \tilde{\zeta}_{2,8} & 0 \\ * & * & \tilde{\zeta}_{3,3} & 0 & \tilde{\zeta}_{3,5} & 0 & 0 & 0 & 0 \\ * & * & * & \tilde{\zeta}_{4,4} & 0 & 0 & \tilde{\zeta}_{4,7} & 0 & 0 \\ * & * & * & * & \tilde{\zeta}_{5,5} & \tilde{\zeta}_{5,6} & 0 & 0 & 0 \\ * & * & * & * & * & \tilde{\zeta}_{6,6} & 0 & 0 & 0 \\ * & * & * & * & * & * & \tilde{\zeta}_{7,7} & 0 & 0 \\ * & * & * & * & * & * & * & \tilde{\zeta}_{8,8} & 0 \\ * & * & * & * & * & * & * & * & \tilde{\zeta}_{9,9} \end{bmatrix} < 0, \tag{10}$$

$\tilde{\zeta}_{1,1} = L\bar{Q}_1 L + \bar{V} + d\bar{M} - \frac{1}{d+\delta_d}[\bar{N} + \frac{\pi^2 \bar{N}}{4}] + \frac{d^2}{2}\bar{Z} - 2\bar{Z} - J_1\bar{G}_1;$

$\tilde{\zeta}_{1,3} = -\frac{1}{d+\delta_d}[\bar{N} + \frac{\pi^2 \bar{N}}{4}];\quad \tilde{\zeta}_{1,4} = \bar{B} - \Gamma^T X^T + Y^T R^T;\quad \tilde{\zeta}_{1,5} = \frac{\pi^2 \bar{N}}{2d^2+\delta_d} + \frac{2\bar{Z}}{d+\delta_d};$

$\tilde{\zeta}_{1,7} = J_2\bar{G}_1;\ \tilde{\zeta}_{2,2} = -(1-\sigma)L\bar{Q}_1 L - J_1\bar{G}_2;\ \tilde{\zeta}_{2,8} = J_2\bar{G}_2;$

$\tilde{\zeta}_{3,3} = -\bar{V} - \frac{1}{d+\delta_d}[\bar{N} + \frac{\pi^2 \bar{N}}{4}];\ \tilde{\zeta}_{3,5} = \frac{\pi^2 \bar{N}}{2d^2+\delta_d};$

$\tilde{\zeta}_{4,4} = d\bar{N} - 2X;\ \tilde{\zeta}_{4,7} = XE;\quad \tilde{\zeta}_{4,8} = XH;$

$\tilde{\zeta}_{5,5} = -\frac{4}{d+\delta_d}\bar{M} - \frac{\pi^2 \bar{N}}{d^3+\delta_d} - \frac{2\bar{Z}}{d^2+\delta_d};\ \tilde{\zeta}_{5,6} = \frac{6}{d^2+\delta_d}\bar{M};\quad \tilde{\zeta}_{6,6} = -\frac{12}{d^3+\delta_d}\bar{M};$

$\tilde{\zeta}_{7,7} = \bar{Q}_2 - \bar{G}_1;\quad \tilde{\zeta}_{8,8} = -(1-\sigma)\bar{Q}_2 - \bar{G}_2;\quad \tilde{\zeta}_{9,9} = -\lambda I;$

Furthermore, the designed memristor-based reliable state-feedback controller (7) gain matrix is given as $K = YX^{-1}$.

PROOF Let us construct the switched system with the help of memristors as

$$\dot{\upsilon}_i(\theta) \in -\Gamma_i \upsilon_i(\theta) + \sum_{i=1}^{n} e_{ij}(\theta)\tilde{g}(\upsilon(\theta)) + \sum_{i=1}^{n} h_{ij}(\theta)\tilde{g}(\upsilon(\theta - d(\theta))) + u_i(\theta). \tag{11}$$

Let us construct the general LKF with the aim of obtaining the outcomes as

$$V(\theta, \upsilon(\theta)) = \sum_{i=1}^{4} V_i(\theta, \upsilon(\theta)), \tag{12}$$

where

$$
\begin{aligned}
V_1(\theta,\upsilon(\theta)) &= \upsilon^T(\theta)B\upsilon(\theta)+\int_{\theta-d}^{\theta}\upsilon^T(s)V\upsilon(s)\,ds,\\
V_2(\theta,\upsilon(\theta)) &= \int_{\theta-d(\theta)}^{\theta}\upsilon^T(s)LQ_1L\upsilon(s)\,ds+\int_{\theta-d(\theta)}^{\theta}\tilde{g}^T(\upsilon(s))Q_2\tilde{g}(\upsilon(s))\,ds,\\
V_3(\theta,\upsilon(\theta) &= \int_{-d}^{0}\int_{\theta+u}^{\theta}\upsilon^T(s)M\upsilon(s)ds\,du+\int_{-d}^{0}\int_{\theta+u}^{\theta}\dot{\upsilon}^T(s)N\dot{\upsilon}(s)ds\,du,\\
V_4(\theta,\upsilon(\theta)) &= \int_{-d}^{0}\int_{u_1}^{\theta}\int_{\theta+u_2}^{\theta}\upsilon^T(s)Z\upsilon(s)ds\,du_1\,du_2.
\end{aligned}
$$

By estimating the time derivative of $V_i(\theta,\upsilon(\theta))$ for the state trajectories of the system (8), we obtain

$$
\dot{V}_1(\theta,\upsilon(\theta))=2\upsilon^T(\theta)B\dot{\upsilon}(\theta)+\upsilon^T(\theta)V\upsilon(\theta)-\upsilon^T(\theta-d)V\upsilon(\theta-d), \tag{13}
$$

$$
\begin{aligned}
\dot{V}_2(\theta,\upsilon(\theta)) &= \upsilon^T(\theta)LQ_1L\upsilon(\theta)-(1-\sigma)\upsilon^T(\theta-d(\theta))LQ_1L\upsilon(\theta-d(\theta))\\
&\quad+\tilde{g}^T(\upsilon(\theta))Q_2\tilde{g}(\upsilon(\theta))-(1-\sigma)\tilde{g}^T(\upsilon(\theta-d(\theta)))Q_2\tilde{g}(\upsilon(\theta-d(\theta))), \qquad (14)\\
\dot{V}_3(\theta,\upsilon(\theta)) &= d\upsilon^T(\theta)M\upsilon(\theta)+d\dot{\upsilon}^T(\theta)N\dot{\upsilon}(\theta)-\int_{\theta-d}^{\theta}\upsilon^T(s)M\upsilon(s)\,ds\\
&\quad-\int_{\theta-d}^{\theta}\dot{\upsilon}^T(s)N\dot{\upsilon}(s)\,ds, \qquad (15)\\
\dot{V}_4(\theta,\upsilon(\theta)) &= \frac{d^2}{2}[\upsilon^T(\theta)Z\upsilon(\theta)]-\int_{-d}^{0}\int_{\theta+u}^{\theta}\upsilon^T(s)Z\upsilon(s)\,ds\,d\theta. \qquad (16)
\end{aligned}
$$

Now, by applying Lemmas 1, 2 and 3, we get

$$
\begin{aligned}
-\int_{\theta-d}^{\theta}\upsilon^T(s)M\upsilon(s)ds &\le -\frac{1}{d+\delta_d}\Big(\int_{\theta-d}^{\theta}\upsilon(s)ds\Big)^T M\Big(\int_{\theta-d}^{\theta}\upsilon(s)ds\Big)\\
&\quad-\frac{3}{d+\delta_d}\Big(\int_{\theta-d}^{\theta}\upsilon(s)\,ds-\frac{2}{d+\delta_d}\int_{\theta-d}^{\theta}\int_{s}^{\theta}\upsilon(u)\,du\,ds\Big)^T M\\
&\quad\times\Big(\int_{\theta-d}^{\theta}\upsilon(s)\,ds-\frac{2}{d+\delta_d}\int_{\theta-d}^{\theta}\int_{s}^{\theta}\upsilon(u)\,du\,ds\Big), \qquad (17)
\end{aligned}
$$

$$
\begin{aligned}
-\int_{\theta-d}^{\theta} \dot{\upsilon}^T(\theta)N\dot{\upsilon}(\theta)\,ds \quad \le \quad & -\frac{1}{d+\delta_d}\Big[\upsilon^T(\theta)\Big(N+\frac{\pi^2 N}{4}\Big)\upsilon(\theta) \\
& +2\upsilon^T(\theta)\Big(N+\frac{\pi^2 N}{4}\Big) \\
& \times\upsilon(\theta-d)+\upsilon^T(\theta-d)\Big(N+\frac{\pi^2 N}{4}\Big)\upsilon(\theta-d) \\
& +2\upsilon^T(\theta)\Big(-\frac{\pi^2 N}{2d+\delta_d}\Big)\int_{\theta-d}^{\theta}\upsilon(s)\,ds \\
& +2\upsilon^T(\theta-d)\Big(-\frac{\pi^2 N}{2d+\delta_d}\Big)\int_{\theta-d}^{\theta}\upsilon(s)\,ds \\
& +\int_{\theta-d}^{\theta}\upsilon^T(s)\,ds\Big(\frac{\pi^2 N}{d^2+\delta_d}\Big)\int_{\theta-d}^{\theta}\upsilon(s)\,ds\Big], \quad (18)
\end{aligned}
$$

$$
\begin{aligned}
-\int_{-d}^{0}\int_{\theta+u}^{\theta}\upsilon^T(s)Z\upsilon(s)\,ds\,du \quad \le \quad & -\frac{2}{d^2+\delta_d}\Big[d\upsilon^T(\theta)-\Big(\int_{\theta-d}^{\theta}\upsilon(s)\,ds\Big)^T\Big]Z \\
& \times\Big[d\upsilon(\theta)-\Big(\int_{\theta-d}^{\theta}\upsilon(s)\,ds\Big)\Big]. \qquad (19)
\end{aligned}
$$

To derive a less conservative criterion, a positive diagonal matrix S holds with the zero equation of the form

$$2\dot{\upsilon}^T(\theta)S[-\Gamma\upsilon(\theta)+E\tilde{g}(\upsilon(\theta))+H\tilde{g}(\upsilon(\theta-d(\theta)))+\hat{u}(\theta)-\dot{\upsilon}(\theta)]=0. \quad (20)$$

Under hypothesis (H2), for any $i=1,2,\cdots,n$ we have

$$(\tilde{g}_i(\upsilon_i(\theta))-J_i^-\upsilon_i(\theta))(\tilde{g}_i(\upsilon_i(\theta))-J_i^+\upsilon_i(\theta))\le 0.$$

Let us consider $G_1=\mathrm{diag}\{g_{11},g_{12},\ldots,g_{1n}\}$, $G_2=\mathrm{diag}\{g_{21},g_{22},\ldots,g_{2n}\}$. Then,

$$\sum_{i=1}^{n} g_{1i}\begin{bmatrix}\upsilon(\theta)\\ \tilde{g}(\upsilon(\theta))\end{bmatrix}^T\begin{bmatrix}J_i^-J_i^+e_ie_i^T & -\frac{J_i^-+J_i^+}{2}e_ie_i^T\\ -\frac{J_i^-+J_i^+}{2}e_ie_i^T & e_ie_i^T\end{bmatrix}\begin{bmatrix}\upsilon(\theta)\\ \tilde{g}(\upsilon(\theta))\end{bmatrix}\le 0, \quad (21)$$

where e_i is used to identify the units as the element values for a column vector, on its i^{th} row, with zeros elsewhere. Equivalently, formula (21) can be of the form

$$\begin{bmatrix}\upsilon(\theta)\\ \tilde{g}(\upsilon(\theta))\end{bmatrix}^T\begin{bmatrix}J_1G_1 & -J_2G_1\\ * & G_1\end{bmatrix}\begin{bmatrix}\upsilon(\theta)\\ \tilde{g}(\upsilon(\theta))\end{bmatrix}\le 0. \qquad (22)$$

Similarly,

$$\begin{bmatrix} \upsilon(\theta - d(\theta)) \\ \tilde{g}(\upsilon(\theta - d(\theta))) \end{bmatrix}^T \begin{bmatrix} J_1 G_2 & -J_2 G_2 \\ * & G_2 \end{bmatrix} \begin{bmatrix} \upsilon(\theta - d(\theta)) \\ \tilde{g}(\upsilon(\theta - d(\theta))) \end{bmatrix} \leq 0. \tag{23}$$

Combining (13) through (23), we obtain

$$\dot{V}(\theta, \upsilon(\theta)) - 2\tilde{g}^T(\upsilon(\theta))u(\theta) - \lambda u^T(\theta)u(\theta) \leq \imath^T(\theta)\,\tilde{\zeta}\,\imath(\theta), \tag{24}$$

where

$$\imath^T(\theta) = \Big[\upsilon^T(\theta) \quad \upsilon^T(\theta - d(\theta)) \quad \upsilon^T(\theta - d) \quad \dot{\upsilon}^T(\theta) \quad \int_{\theta-d}^{\theta} \upsilon^T(s)ds \\ \int_{\theta-d}^{\theta}\int_{s}^{\theta} \upsilon^T(s)duds \quad \tilde{g}^T(\upsilon(\theta)) \quad \tilde{g}^T(\upsilon(\theta - d(\theta))) \quad u^T(\theta)\Big].$$

Therefore, if LMI (10) holds, we deduce in the following manner

$$\dot{V}(\theta, \upsilon(\theta)) - 2\tilde{g}^T(\upsilon(\theta))u(\theta) - \lambda u^T(\theta)u(\theta) \leq 0. \tag{25}$$

Integration takes place for the equation (25) with time interval $[0, \theta_\upsilon]$, and so, we get

$$2\int_0^{\theta_\upsilon} \bar{g}^T(\upsilon(s))u(s)\,ds \geq V(\theta_\upsilon, \upsilon(\theta_\upsilon)) - V(0, \upsilon(0)) - \lambda u^T(s)u(s)\,ds, \tag{26}$$

and for $\upsilon(0) = 0$, we have $V(0, \upsilon(0)) = 0$. We apply the congruence transformation $S = X^{-1}$, the control transformation $K = YX^{-1}$, and the matrix variables $\bar{B} = \upsilon\, B\, \upsilon$, $\bar{V} = \upsilon\, V\, \upsilon$, $\bar{Q}_r = \upsilon\, Q_r\, \upsilon$, $\bar{M} = \upsilon\, M\, \upsilon$, $\bar{Z} = \upsilon\, Z\, \upsilon$, $\bar{N} = \upsilon\, N\, \upsilon$ and $\bar{G}_r = \upsilon\, G_r\, \upsilon$, and we write $\upsilon\, J_r G_r\, \upsilon$ as $J_r \upsilon\, G_r\, \upsilon$ where $r = 1, 2$. Therefore, in accordance with (10), we have $\dot{V}(\theta, \upsilon(\theta)) \leq 0$ for $\imath(\theta) \neq 0$ and by utilizing Lyapunov theory and definition (1), the scrutinized MNNs of (3) guarantees passivity for the state-dependent switched systems. Hence the proof. ∎

Remark 3 *In equation* (25)*, when the value of* λ *and activation functions are zero, then we achieve the fulfilment of asymptotic stability criteria.*

In the next theorem, we explore the failure matrix R, where un-fixed shortages happens, but still satisfies the restraints in (6), then the reliable state-feedback controller is applied for subsequent theorems based on the conditions provided in Theorem 1 for switched system to be passive.

Theorem 2 *Under hypothesis (H2) and for any given positive scalars* d*,* σ *and* ϵ*, the MNNs system* (3) *is passive in the presence of unknown actuator failure* *matrix R, if there exist positive definite matrices* $\bar{B} > 0$, $\bar{V} > 0$, $\bar{Q}_1 > 0$, $\bar{Q}_2 > 0$, $\bar{M} > 0$, $\bar{N} > 0$ *and* $\bar{Z} > 0$, *diagonal matrices* $\bar{G}_1 > 0$, $\bar{G}_2 > 0$ *and real matrices* S, Y, *with appropriate dimensions. Then, the following LMIs hold:*

$$\begin{bmatrix} \tilde{\zeta} & \tilde{Y}\breve{R} & \epsilon\tilde{I} \\ * & -\epsilon & 0 \\ * & * & -\epsilon \end{bmatrix} < 0. \tag{27}$$

Moreover, the formulatio of the LMI terms for $\tilde{\zeta}$ *follows the specifications, provided in Theorem 1. Then, the designed reliable state-feedback controller gain matrix* $K = YX^{-1}$ *for the system* (7) *is obtained.*

Proof Let us consider the constraints from equation (6), where the actuator fault matrix R is not known accurately. Next, we construct the matrix ζ with the same parameters as per Theorem 1. Hence, the matrix $\tilde{\zeta}$ can be noted in the following manner

$$\breve{\zeta} = \tilde{\zeta} + \tilde{I}\Theta\tilde{Y} + \tilde{Y}^T\Theta\tilde{I}^T,$$

where $\tilde{I} = [I \;\; 0_{n,8n}]$, $\tilde{Y} = [0_{n,4n}\, Y\, 0_{n,4n}]$. Then, by choosing a positive scalar $\epsilon > 0$, we obtain $\tilde{\zeta}$ by replacing R by $\breve{R}$ in LMI (10). By applying Lemma 4, it is easy to form the matrix as

$$\breve{\zeta} \leq \tilde{\zeta} + \epsilon\tilde{I}^T\tilde{I} + \epsilon^{-1}\tilde{Y}\breve{R}\tilde{Y}^T, \tag{28}$$

so that we obtain that (28) is equivalent to LMI (27). Therefore, this confirms that the considered MNN system (3) is passive under the state-dependent switching system. The proof is complete. ∎

Remark 4 *Internal stability state ensures the passivity property. By making use of the switching law on feedback interconnections, it is possible to extract a gain matrix accuracy for both linear and non-linear systems. Passivity deals with results based on the analogy between stability and passivity of non-linear models (see Guo, Wang and Yan, 2014; Huang, Qiu and Ren, 2020; Shafiya and Nagamani, 2022; Xiao and Zheng, 2020; Song and Wang, 2010; Ge et al., 2016).*

In the next subsection, some sufficient condition are addressed under continuous law for passivity property for the known and unknown actuator cases. This is possible only by making use of the features of memristor together with NNs, so that we can get invariant outcomes based on continuous memductance approach.

3.2. State-dependent continuous MNNs

In the following theorem, we consider the state-dependent continuous system, meant to be passive for the known failure matrix R, based on MNNs with time-varying delay.

Theorem 3 *Under hypothesis (H2) and for given scalars d and σ, the MNNs system* (3) *is passive in the presence of known actuator fault R, if there exist positive definite matrices $\bar{B} > 0$, $\bar{V} > 0$, $\bar{Q}_1 > 0$, $\bar{Q}_2 > 0$, $\bar{M} > 0$, $\bar{N} > 0$ and $\bar{Z} > 0$, diagonal matrices $\bar{G}_1 > 0$, $\bar{G}_2 > 0$, real matrices S, Y, with appropriate dimensions, and then the following LMIs holds for the below specified LMI:*

$$\tilde{\zeta} = \begin{bmatrix} \tilde{\zeta}_{1,1} & 0 & \tilde{\zeta}_{1,3} & \tilde{\zeta}_{1,4} & \tilde{\zeta}_{1,5} & 0 & 0 \\ * & \tilde{\zeta}_{2,2} & 0 & \tilde{\zeta}_{2,4} & 0 & 0 & 0 \\ * & * & \tilde{\zeta}_{3,3} & 0 & \tilde{\zeta}_{3,5} & 0 & 0 \\ * & * & * & \tilde{\zeta}_{4,4} & 0 & 0 & 0 \\ * & * & * & * & \bar{\xi}_{5,5} & 0 & 0 \\ * & * & * & * & * & \tilde{\zeta}_{6,6} & 0 \\ * & * & * & * & * & * & \tilde{\zeta}_{7,7} \end{bmatrix} < 0, \tag{29}$$

$\tilde{\zeta}_{1,1} = \bar{V} + L[\bar{Q}_1 + \bar{Q}_2]L + d\bar{M} - \frac{1}{d+\delta_d}[\bar{N} + \frac{\pi^2\bar{N}}{4}] + \frac{d^2}{2}\bar{Z} - 2\bar{Z};$

$\tilde{\zeta}_{1,3} = -\frac{1}{d+\delta_d}[\bar{N} + \frac{\pi^2\bar{N}}{4}];$ $\quad \tilde{\zeta}_{1,4} = \bar{B} - (X\Gamma)^T + Y^T R^T + X^T(\Xi H)^T;$

$\tilde{\zeta}_{1,5} = \frac{\pi^2\bar{N}}{2d^2+\delta_d} + \frac{2\bar{Z}}{d+\delta_d};$ $\quad \tilde{\zeta}_{2,2} = -(1-\sigma)L[\bar{Q}_1 + \bar{Q}_2]L;$ $\quad \tilde{\zeta}_{2,4} = X^T(\Upsilon H)^T;$

$\tilde{\zeta}_{3,3} = -\bar{V} - \frac{1}{d+\delta_d}[\bar{N} + \frac{\pi^2\bar{N}}{4}];$ $\quad \tilde{\zeta}_{3,5} = \frac{\pi^2\bar{N}}{2d^2+\delta_d};$ $\quad \tilde{\zeta}_{4,4} = d\bar{N} - 2X;$

$\tilde{\zeta}_{5,5} = -\frac{4}{d+\delta_d}\bar{M} - \frac{\pi^2\bar{N}}{d^3+\delta_d} - \frac{2\bar{Z}}{d^2+\delta_d};$ $\quad \tilde{\zeta}_{5,6} = \frac{6}{d^2+\delta_d}\bar{M};$ $\quad \tilde{\zeta}_{6,6} = -\frac{12}{d^2+\delta_d}\bar{M};$

$\tilde{\zeta}_{7,7} = -\lambda I;$

Furthermore, for the designed memristor-based reliable state-feedback controller (7)*, the gain matrix is given as $K = YX^{-1}$.*

Proof For constructing the continuous passive case consider the equation (3) to show the following equation:

$$\dot{\upsilon}_i(\theta) \in -\Gamma_i\upsilon_i(\theta) + \sum_{i=1}^{n} \Xi|\tilde{g}(\upsilon(\theta))| + \sum_{i=1}^{n} \Upsilon|\tilde{g}(\upsilon(\theta - d(\theta)))| + u_i(\theta). \tag{30}$$

In terms of modifying (30) into a compact form

$$\dot{\upsilon}(\theta) \leq -\Gamma\upsilon(\theta) + \Xi|\tilde{g}(\upsilon(\theta))| + \Upsilon|\tilde{g}(\upsilon(\theta - d(\theta)))| + u(\theta). \tag{31}$$

By using the LKF in Theorem 1 and combining it with Case 2a, we get

$$\begin{aligned}\dot{V}_2(\theta,\upsilon(\theta)) &= \upsilon^T(\theta)LQ_1L\upsilon(\theta)-(1-\sigma)\upsilon^T(\theta-d(\theta))LQ_1L\upsilon(\theta-d(\theta))\\ &\quad+\tilde{g}^T(\upsilon(\theta))Q_2\tilde{g}(\upsilon(\theta))-(1-\sigma)\tilde{g}^T(\upsilon(\theta-d(\theta)))Q_2\tilde{g}(\upsilon(\theta-d(\theta))),\\ &\leq \upsilon^T(\theta)[L(Q_1+Q_2)L]\upsilon(\theta)-(1-\sigma)[\upsilon^T(\theta-d(\theta))][L(Q_1+Q_2)L]\\ &\quad\upsilon(\theta-d(\theta)). \end{aligned}\tag{32}$$

At the same time, by calculating the time derivatives $V_i(\theta,\upsilon(\theta))$ for $i=1,3,4$ as derived terms in Theorem 1 and applying differential inclusion theory and set-valued map directly, without Filipov solutions, the resulting system exhibits continuous behavior, instead of the discontinuous switching, present in Case 2a. Consider a slack matrix S with the less conservative criterion holding as

$$2\dot{\upsilon}^T(\theta)S[-\Gamma\upsilon(\theta)+\Xi\tilde{g}(\upsilon(\theta))+\Upsilon\bar{g}(\upsilon(\theta-d(\theta)))+\hat{u}(\theta)-\dot{\upsilon}(\theta)]=0. \tag{33}$$

Then, it is easy to get that

$$\dot{V}(\theta,\upsilon(\theta))-2\tilde{g}^T(\upsilon(\theta))u(\theta)-\lambda u^T(\theta)u(\theta)\leq \imath^T(\theta)\,\zeta\,\imath(\theta), \tag{34}$$

where

$$\begin{aligned}\imath^T(\theta)=\Big[\upsilon^T(\theta)\qquad \upsilon^T(\theta-d(\theta))\qquad \upsilon^T(\theta-d)\qquad \dot{\upsilon}^T(\theta)\int_{\theta-d}^{\theta}\upsilon^T(s)ds\\ \int_{\theta-d}^{\theta}\int_s^{\theta}\upsilon^T(s)duds\qquad u^T(\theta)\Big].\end{aligned}$$

Therefore, if the LMI (29) holds, then

$$\dot{V}(\theta,\upsilon(\theta))-2\tilde{g}^T(\upsilon(\theta))u(\theta)-\lambda u^T(\theta)u(\theta)\leq 0. \tag{35}$$

Next, integration takes place for equation (35) with its range of time being the interval $[0,\theta_\upsilon]$, so that

$$2\int_0^{\theta_\upsilon}\tilde{g}^T(\upsilon(s))u(s)\,ds\geq V(\theta_\upsilon,\upsilon(\theta_\upsilon))-V(0,\upsilon(0))-\lambda u^T(s)u(s)\,ds, \tag{36}$$

for $\upsilon(0)=0$, we have $V(0,\upsilon(0))=0$, and we apply a congruence transformation to obtain the gain matrices by $X^{-1}=S$, $\bar{B}=\upsilon\,B\,\upsilon$, $\bar{V}=\upsilon\,V\,\upsilon$, $\bar{Q}_r=\upsilon\,Q_r\upsilon$, $\bar{M}=\upsilon\,M\,\upsilon$, $\bar{Z}=\upsilon\,Z\,\upsilon$, $\bar{N}=\upsilon\,N\,\upsilon$, where $r=1,2$. By implementing the controller gain matrix, $K=YX^{-1}$. Therefore, we deduce from (29) that $\dot{V}(\theta,\upsilon(\theta))\leq 0$ for $\imath(\theta)\neq 0$. Furthermore, based on definition (1), the analyzed MNN system (3) exhibits passivity into the context of the state-dependent continuous system. Hence the proof. ■

Next, we formulate the continuous law of memristor based state-dependent continuous system under the original passivity property for reliable state-feedback controller, when actuator faults are unknown.

Theorem 4 *Under hypothesis (H2) and for any given positive scalars d, σ and ϵ, the MNNs system* (3) *is said to be passive in the presence of unknown actuator failure matrix R, if there exist positive definite matrices $\bar{B} > 0$, $\bar{V} > 0$, $\bar{Q}_1 > 0$, $\bar{Q}_2 > 0$, $\bar{M} > 0$, $\bar{N} > 0$ and $\bar{Z} > 0$, diagonal matrices $\bar{G}_1 > 0$, $\bar{G}_2 > 0$ and real matrices S, Y with appropriate dimensions, along with reliable controller* (7) $K = YX^{-1}$ *is achieved. Then the following linear matrix inequality holds*

$$\begin{bmatrix} \tilde{\zeta} & \tilde{Y}\check{R} & \epsilon\tilde{I} \\ * & -\epsilon & 0 \\ * & * & -\epsilon \end{bmatrix} < 0, \tag{37}$$

and, additionally, the remaining LMI terms of $\tilde{\zeta}$ are zero as specified in Theorem 3.

Proof Let us consider the constraints from equation (6), where the actuator fault matrix R is not known exactly. Next, we construct the matrix ζ with the same parameters as in Theorem 3. Hence, the matrix ζ can be written down in the following form

$$\check{\zeta} = \tilde{\zeta} + \tilde{I}\Theta\tilde{Y} + \tilde{Y}^T\Theta\tilde{I}^T,$$

where $\tilde{I} = [I \ \ 0_{n,6n}]$, $\tilde{Y} = [0_{n,3n}\, Y\, 0_{n,3n}]$. Then, by choosing a positive scalar $\epsilon > 0$, we obtain $\tilde{\zeta}$ by replacing R by $\check{R}$ in LMI (29). By applying Lemma 4, it is easy to form the matrix as

$$\check{\zeta} \leq \tilde{\zeta} + \epsilon\tilde{I}^T\tilde{I} + \epsilon^{-1}\tilde{Y}\check{R}\tilde{Y}^T, \tag{38}$$

where the obtained (38) is equivalent to LMI (37). Therefore, this proves that the analysed MNNs (3) is passive for state-dependent continuous system. Thus, the proof is complete. ■

Remark 5 *In this study, authors examined MNNs with different memductance functions, which is the state-dependent switching system, or a state-dependent continuous system that is a generalization of the analysis for the traditional artificial neural networks presented in Wu and Zeng (2014). Let us look into the significant distinctions of our proposed work compared with that of the aforementioned literature. First and foremost, a non-smooth analysis of differential inclusion theory and set valued maps has been used in this proposed study, so that an advance could be presented, while deriving LKFs through the utilization of Wirtinger's inequality, Jensen's inequality, and Schur complement* *lemma, whereas the mentioned reference deals with the basic lemma. Then, the reliable stabilizing controller law is exhibited for both known and unknown cases of actuator fault whereas the cited reference lacks controller design. Further, chaotic behavior in general might occur in the context of the MNN model and we have shown the chaotic performance for the passivity criterion for the here presented new results,, while chaotic performance is not considered in Wu and Zeng (2014). Only few results on the passivity of memductance approach–based systems were found in the existing literature that dealt with using various paradigms including BAMNNs (Anbuvithya et al., 2016), and MNNs (Liu and Xu, 2016). It is possible to examine many different kinds of NNs using the technique described in this paper.*

REMARK 6 *It is worth noting that Theorems 1 and 3 are derived for normal and fixed actuator failure case, while Theorems 2 and 4 are derived for unknown time varying actuator failure case for non-identical memductance functions.*

REMARK 7 *The stability and synchronization of highly complex NNs can be comprehensively evaluated through the application of passivity theory. In addressing the actuator fault dynamics, the implementation of a state-feedback controller provides more refined, less conservative outcomes, enhancing the feasibility of MNNs through the strategic use of Wirtinger's inequality and Jensen's inequality.*

REMARK 8 *In general, chaotic systems might give a glimpse of the way to generate random numbers, such deterministic systems may have a time evolution that seems very irregular and possesses the usual characteristics of actual random processes.*

4. Numerical simulations

In this section, we provide a simulation analysis for the memductance approach based on actuator fault for state-dependent switched and continuous cases for passivity in order to illustrate results here formulated.

EXAMPLE 1 *Consider the following two-dimensional switched MNNs with actuator fault cases*

$$\begin{bmatrix} \dot{\upsilon}_1(\theta) \\ \dot{\upsilon}_2(\theta) \end{bmatrix} = \begin{bmatrix} -\Gamma_{11} & 0 \\ 0 & -\Gamma_{22} \end{bmatrix} \begin{bmatrix} \upsilon_1(\theta) \\ \upsilon_2(\theta) \end{bmatrix} + \begin{bmatrix} e_{11}(\upsilon_1(\theta)) & e_{12}(\upsilon_1(\theta)) \\ e_{21}(\upsilon_2(\theta)) & e_{22}(\upsilon_2(\theta)) \end{bmatrix} \begin{bmatrix} \tilde{g}_1(\upsilon_1(\theta)) \\ \tilde{g}_2(\upsilon_2(\theta)) \end{bmatrix}$$
$$+ \begin{bmatrix} h_{11}(\upsilon_1(\theta)) & h_{12}(\upsilon_1(\theta)) \\ h_{21}(\upsilon_2(\theta)) & h_{22}(\upsilon_2(\theta)) \end{bmatrix} \begin{bmatrix} \tilde{g}_1(\upsilon_1(\theta - d(\theta))) \\ \tilde{g}_2(\upsilon_2(\theta - d(\theta))) \end{bmatrix} + \begin{bmatrix} u_1(\theta) \\ u_2(\theta) \end{bmatrix}, \tag{39}$$

where

$$e_{11}(\upsilon_1(\theta)) = \begin{cases} -0.16, & |\upsilon_1(\theta)| \le 2, \\ 0.16, & |\upsilon_1(\theta)| > 2, \end{cases} \quad e_{12}(\upsilon_1(\theta)) = \begin{cases} -0.34, & |\upsilon_1(\theta)| \le 2, \\ 0.34, & |\upsilon_1(\theta)| > 2, \end{cases}$$

$$e_{21}(\upsilon_2(\theta)) = \begin{cases} -0.51, & |\upsilon_2(\theta)| \le 2, \\ 0.51, & |\upsilon_2(\theta)| > 2, \end{cases} \quad e_{22}(\upsilon_2(\theta)) = \begin{cases} -0.52, & |\upsilon_2(\theta)| \le 2, \\ 0.52, & |\upsilon_2(\theta)| > 2, \end{cases}$$

$$h_{11}(\upsilon_1(\theta)) = \begin{cases} -0.17, & |\upsilon_1(\theta)| \le 2, \\ 0.17, & |\upsilon_1(\theta)| > 2, \end{cases} \quad h_{12}(\upsilon_1(\theta)) = \begin{cases} -0.55, & |\upsilon_1(\theta)| \le 2, \\ 0.55, & |\upsilon_1(\theta)| > 2, \end{cases}$$

$$h_{21}(\upsilon_2(\theta)) = \begin{cases} -0.55, & |\upsilon_2(\theta)| \le 2, \\ 0.55, & |\upsilon_2(\theta)| > 2, \end{cases} \quad h_{22}(\upsilon_2(\theta)) = \begin{cases} -0.48, & |\upsilon_2(\theta)| \le 2, \\ 0.48, & |\upsilon_2(\theta)| > 2. \end{cases}$$

Let us select the activation function in the following form:

$\tilde{g}(\upsilon(\theta)) = \begin{bmatrix} \tanh(0.95.\upsilon_1(\theta)) \\ \tanh(0.95.\upsilon_2(\theta)) \end{bmatrix}$ and from Hypothesis (H2), $J_1 = diag\{0, 0\}$, $J_2 = diag\{0.5, 0.6\}$ is applied for all three cases, that is (1) normal, (2) fixed and (3) unknown actuator cases. MNNs can be used to forecast simulation accuracy, which allows us to experimentally investigate the nature of chaotic phenomena. MNNs can predict how closely a simulation will match the real or expected behavior. We derived the results analytically using LMI technique and congruence transformation, while simulation results are obtained based on LMI control toolbox:

$$B = \begin{bmatrix} 1.7592 & -0.0000 \\ -0.0000 & 1.7592 \end{bmatrix}, Q_1 = \begin{bmatrix} 2.6035 & -0.0826 \\ -0.0826 & 2.1667 \end{bmatrix}, Q_2 = \begin{bmatrix} 0.8637 & 0.0285 \\ 0.0285 & 0.7118 \end{bmatrix},$$

$$M = \begin{bmatrix} 0.2443 & -0.0134 \\ -0.0134 & 0.2257 \end{bmatrix}, Z = \begin{bmatrix} 0.7662 & -0.0449 \\ -0.0449 & 0.8023 \end{bmatrix}, V = \begin{bmatrix} 0.5144 & -0.0786 \\ -0.0786 & 0.4123 \end{bmatrix},$$

$$N = \begin{bmatrix} 0.7237 & -0.0475 \\ -0.0475 & 0.7623 \end{bmatrix}, X = \begin{bmatrix} 0.9028 & 0 \\ 0 & 0.9459 \end{bmatrix}, Y = \begin{bmatrix} -2.3275 & -0.2652 \\ -0.3512 & -2.6453 \end{bmatrix},$$

Here, we adopt the stabilizing control law, in order to achieve the passivity results for the switched case via reliable state-feedback controller depending on actuator fault matrices. Let us consider the specified below three different cases of model (1) to exhibit the valid simulations on actuators for the essential results, provided here. First of all, the initial values of the state variables are chosen in the random manner.

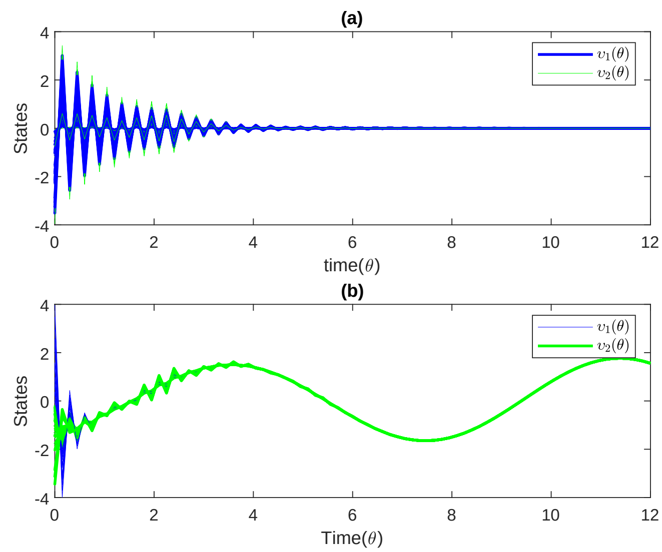

Figure 1: (a) Passive trajectories of switched normal actuator (40) under control. (b) Passive trajectories of switched normal actuator (40) not under control (representation of actuator fault $R = I$)

(i) Switched normal actuator

Let us construct the system (39) by applying the suitable control inputs, observe the inherent performance of the switched normal actuator fault performance

$$\begin{bmatrix}\dot{\upsilon}_1(\theta)\\ \dot{\upsilon}_2(\theta)\end{bmatrix} = \begin{bmatrix}-0.5 & 0\\ 0 & -0.5\end{bmatrix}\begin{bmatrix}\upsilon_1(\theta)\\ \upsilon_2(\theta)\end{bmatrix} + \begin{bmatrix}0.16 & 0.34\\ 0.51 & 0.52\end{bmatrix}\begin{bmatrix}\tilde{g}_1(\upsilon_1(\theta))\\ \tilde{g}_2(\upsilon_2(\theta))\end{bmatrix} + \begin{bmatrix}0.17 & 0.55\\ 0.55 & 0.48\end{bmatrix}\begin{bmatrix}\tilde{g}_1(\upsilon_1(\theta - d(\theta)))\\ \tilde{g}_2(\upsilon_2(\theta - d(\theta)))\end{bmatrix} + IK\begin{bmatrix}\upsilon_1(\theta)\\ \upsilon_2(\theta)\end{bmatrix}, \tag{40}$$

Generally, a normal actuator ensures a robust stability state of the respective models. In general, occurrence of failures in such paradigms is not possible. We constructed a normal case to demonstrate the visually obvious simulation effects at the initial stage of model behavior. In order to perform the theoretical and graphical simulation analysis, let us first assume the known state-feedback reliable actuator faults for the normal case to be $R = I$ with uncertain parametric delay $\delta_d = 0.05$. Next, we proceed with the system dynamics under derivative $\sigma = 0.03$, and time-varying bound, characterized by $d = 0.03$. From Theorem

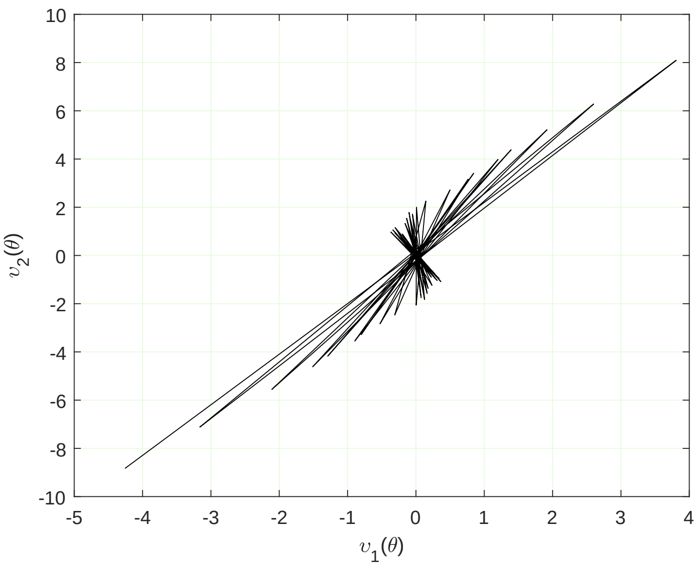

Figure 2: Chaotic behavior of switched normal actuator fault

1, the passivity performance index $\lambda = 1.7592$ can be obtained by making use of MATLAB LMI control toolbox. To ensure stability in switched actuator configurations of established passivity criteria and reliable state-feedback controls were implemented, with corresponding feasible controller matrices as provided below:

$$K = \begin{bmatrix} -2.5780 & -0.2804 \\ -0.3890 & -2.7967 \end{bmatrix}.$$

It is obvious from equation (40) that the trajectories $v_1(\theta)$ and $v_2(\theta)$, shown in Fig. 1 (a) clearly illustrate the stable state convergence of MNNs in the presence of reliable control inputs based on the switched normal actuators to demonstrate the feasible solution of LMIs. Hence, this guarantees that the closed-loop system attains the intended performance, demontrating internal stability under the implemented control framework. Moreover, Fig. 1 (b) shows the explicit behaviour of the trajectories $v_1(\theta)$ and $v_2(\theta)$, if reliable controller is not under control, so that it does not approach the critical point.

(ii) Switched fixed actuator

Let us construct the system (39) by providing a suitable control inputs, to observe the switched fixed actuator fault performance

$$\begin{bmatrix}\dot{\upsilon}_1(\theta)\\ \dot{\upsilon}_2(\theta)\end{bmatrix} = \begin{bmatrix}-0.5 & 0\\ 0 & -0.5\end{bmatrix}\begin{bmatrix}\upsilon_1(\theta)\\ \upsilon_2(\theta)\end{bmatrix} + \begin{bmatrix}0.16 & 0.34\\ 0.51 & 0.52\end{bmatrix}\begin{bmatrix}\tilde{g}_1(\upsilon_1(\theta))\\ \tilde{g}_2(\upsilon_2(\theta))\end{bmatrix} + \begin{bmatrix}0.17 & 0.55\\ 0.55 & 0.48\end{bmatrix}\begin{bmatrix}\tilde{g}_1(\upsilon_1(\theta - d(\theta)))\\ \tilde{g}_2(\upsilon_2(\theta - d(\theta)))\end{bmatrix} + RK\begin{bmatrix}\upsilon_1(\theta)\\ \upsilon_2(\theta)\end{bmatrix}. \tag{41}$$

Actuator faults are common in non-linear systems, with fixed actuators failures typically arising from partial degradation in the system's operation. Even when only a partial failure takes place, it is a difficult task to maintain stable performance within a fixed range of time intervals. Additionally, it is crucial to design a robust state-feedback controller to closely align the theoretical results with realistic simulation outcomes. The actuator fault matrix is supposed to take values in the range of $R = diag\{0.67, 0.54\}$. This can be made possible only by choosing the parameters for the fixed actuator case such as estimated values of derivative $\sigma = 0.03$, the time-varying bound $d = 1.23$ and uncertain delay $\delta_d = 0.05$. The passivity performance index $\lambda = 1.7592$ has been obtained from Theorem 1 with the help of LMI control toolbox. By applying the reliable controller gain matrices to control input, we get a feasible solution of the form

$$K = \begin{bmatrix} -3.8477 & -0.4185\\ -0.7073 & -5.0848\end{bmatrix}.$$

From Fig. 3 (c), we can deduce that even with partial failures in actuators, the trajectories $\upsilon_1(\theta)$ and $\upsilon_2(\theta)$ under reliable state-feedback controller converges and guarantees the internal stability of MNNs following the switched passivity criteria with the help of Wirtinger's and Jensen's inequality based on Lyapunov stability theory. At the same time, Fig. 3 (d) reveals that without reliable state-feedback controller the proposed model is not in the stable mode.

(iii) Switched un-fixed time-varying actuator

Let us construct the system (39) by giving a suitable control inputs, in order to demonstrate the switched un-fixed actuator fault performance

$$\begin{bmatrix}\dot{\upsilon}_1(\theta)\\ \dot{\upsilon}_2(\theta)\end{bmatrix} = \begin{bmatrix}-0.5 & 0\\ 0 & -0.5\end{bmatrix}\begin{bmatrix}\upsilon_1(\theta)\\ \upsilon_2(\theta)\end{bmatrix} + \begin{bmatrix}0.16 & 0.34\\ 0.51 & 0.52\end{bmatrix}\begin{bmatrix}\tilde{g}_1(\upsilon_1(\theta))\\ \tilde{g}_2(\upsilon_2(\theta))\end{bmatrix} + \begin{bmatrix}0.17 & 0.55\\ 0.55 & 0.48\end{bmatrix}\begin{bmatrix}\tilde{g}_1(\upsilon_1(\theta - d(\theta)))\\ \tilde{g}_2(\upsilon_2(\theta - d(\theta)))\end{bmatrix} + \Big(\frac{\hat{R} + \check{R}}{2}\Big)K\begin{bmatrix}\upsilon_1(\theta)\\ \upsilon_2(\theta)\end{bmatrix}. \tag{42}$$

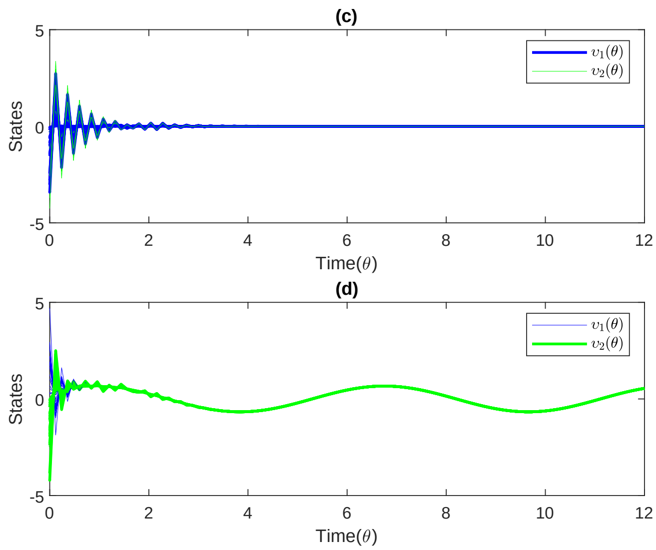

Figure 3: (c) Passive trajectories of the switched fixed actuator system (41) under reliable control outputs. (d) Passive trajectories of the switched fixed actuator system (41) not under reliable control outputs (representation of actuator fault $0 \leq R \leq 1$)

Basically, abnormal malfunctions, external environmental disturbances, noisy input signal might take place unexpectedly in such systems. Even the type of failures that might occur in such a system, such as partial or total failure, is impossible to anticipate. In some situations, actuator components perform well, even though the system is affected by failures. For such cases, we design a reliable controller, functioning in the presence of un-fixed failures in the range of fault matrices bound intervals, which can be defined as $0.53 = \underline{r}_1 \leq r_1 \leq \bar{r}_1 = 0.55$, $0.71 = \underline{r}_2 \leq r_2 \leq \bar{r}_2 = 0.75$, where $R = diag\{0.62, 0.65\}$. Moreover, in order to establish the theoretical results via simulative behaviors, we choose the parameters with estimated values of derivative as follows: $\sigma = 0.03$, the time-varying bound $d = 0.36$ and uncertain delay $\delta_d = 0.04$. The system passivity performance index $\lambda = 2.4874$ is obtained. Then, by utilizing the LMI constrains in Theorem 2 using MATLAB LMI control toolbox, we get reliable controller gain matrix solutions of the form

$$K = \begin{bmatrix} -5.5039 & 0.2998 \\ 0.0728 & -5.1068 \end{bmatrix}.$$

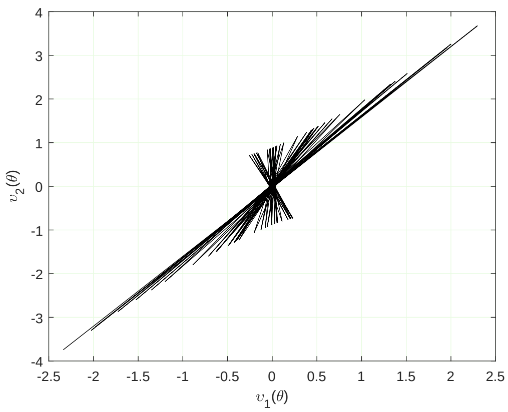

Figure 4: Chaotic behavior of switched fixed actuator fault

In general, by implementing a suitable control technique it is possible to keep the system in the stable state. The graphical simulation implies that the trajectories, obtained under a reliable controller, have good compatibility with un-fixed time-varying MNNs for switched passive system, shown in Fig. 5 (e), by utilizing Lyapunov stability analysis. Regarding the very same point, Fig. 5 (f) illustrates the behavior of trajectories not under control scheme.

In the light of the above, Figs. 1, 3 and 5 show that the designed reliable controller with state variables $\upsilon_1(\theta), \upsilon_2(\theta)$ approaches the equilibrium point zero. The chaotic behavior of switched actuators is also shown in Figs. 2, 4 and 6, respectively. Therefore, it is graphically demonstrated that the MNNs with known and unknown actuators of equations (40), (41) and (4) guarantee that the state-dependent switched system is passive.

Example 2 *Consider a two-dimensional continuous MNN model with actuator fault, as follows*

$$\begin{bmatrix}\dot{\upsilon}_1(\theta)\\ \dot{\upsilon}_2(\theta)\end{bmatrix} = \begin{bmatrix}-0.5 & 0\\ 0 & -0.5\end{bmatrix}\begin{bmatrix}\upsilon_1(\theta)\\ \upsilon_2(\theta)\end{bmatrix} + \begin{bmatrix}e_{11}(\upsilon_1(\theta)) & e_{12}(\upsilon_1(\theta))\\ e_{21}(\upsilon_2(\theta)) & e_{22}(\upsilon_2(\theta))\end{bmatrix}\begin{bmatrix}\tilde{g}_1(\upsilon_1(\theta))\\ \tilde{g}_2(\upsilon_2(\theta))\end{bmatrix}$$
$$+ \begin{bmatrix}h_{11}(\upsilon_1(\theta)) & h_{12}(\upsilon_1(\theta))\\ h_{21}(\upsilon_2(\theta)) & h_{22}(\upsilon_2(\theta))\end{bmatrix}\begin{bmatrix}\tilde{g}_1(\upsilon_1(\theta - d(\theta)))\\ \tilde{g}_2(\upsilon_2(\theta - d(\theta)))\end{bmatrix} + \begin{bmatrix}u_1(\theta)\\ u_2(\theta)\end{bmatrix}. \quad (43)$$

In this section, let us consider extended part of switched case to continuous case for known (normal or fixed actuator) and unknown (time-varying) cases of the model (43) *simulations for three different actuator cases, obtained by implementing the stabilizing control law for the essential outcomes based on*

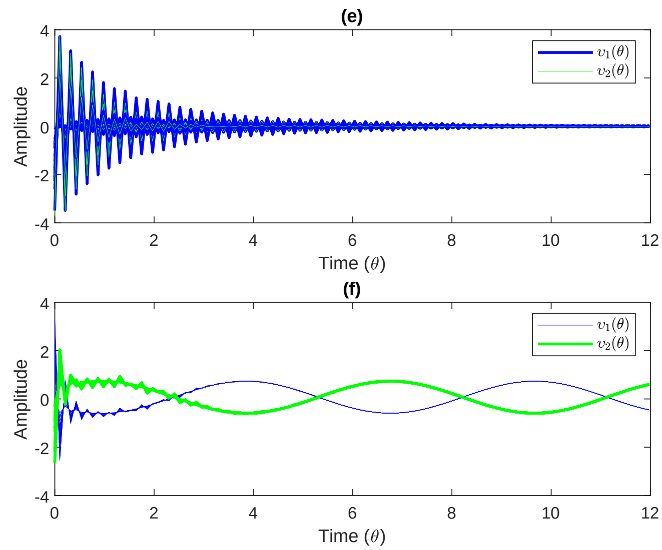

Figure 5: (e) Passive trajectories of switched un-fixed actuator (4) under reliable controller. (f) Passive trajectories of switched un-fixed actuator (4) not under reliable controller (representation of actuator fault when $0 < R < 1$)

Theorems 3 and 4. The initial values of the state variables are chosen in the random manner. The activation functions are chosen to be the same as given in Example 1. Owing to its property of continuity, the system inherently disregards the previous values of the memristive connection weights and updates only the new values, as this is shown in equations (44) through (46).

4.1. (i) Continuous normal actuators

Let us design an ideal controller for the proposed system (43), to observe the known continuous normal actuator fault performance

$$\begin{bmatrix}\dot{\upsilon}_1(\theta)\\ \dot{\upsilon}_2(\theta)\end{bmatrix} = \begin{bmatrix}-0.5 & 0\\ 0 & -0.5\end{bmatrix}\begin{bmatrix}\upsilon_1(\theta)\\ \upsilon_2(\theta)\end{bmatrix} + \begin{bmatrix}-0.1\sin(\upsilon_1(\theta)) & 0.3\cos(\upsilon_1(\theta))\\ 0.2\sin(\upsilon_2(\theta)) & -0.1\cos(\upsilon_2(\theta))\end{bmatrix}\begin{bmatrix}\tilde{g}_1(\upsilon_1(\theta))\\ \tilde{g}_2(\upsilon_2(\theta))\end{bmatrix} + \begin{bmatrix}0.2\sin(\upsilon_1(\theta)) & -0.3\cos(\upsilon_1(\theta))\\ -0.5\sin(\upsilon_2(\theta)) & 0.4\cos(\upsilon_2(\theta))\end{bmatrix}\begin{bmatrix}\tilde{g}_1(\upsilon_1(\theta-d(\theta)))\\ \tilde{g}_2(\upsilon_2(\theta-d(\theta)))\end{bmatrix} + IK\begin{bmatrix}\upsilon_1(\theta)\\ \upsilon_2(\theta)\end{bmatrix}. \tag{44}$$

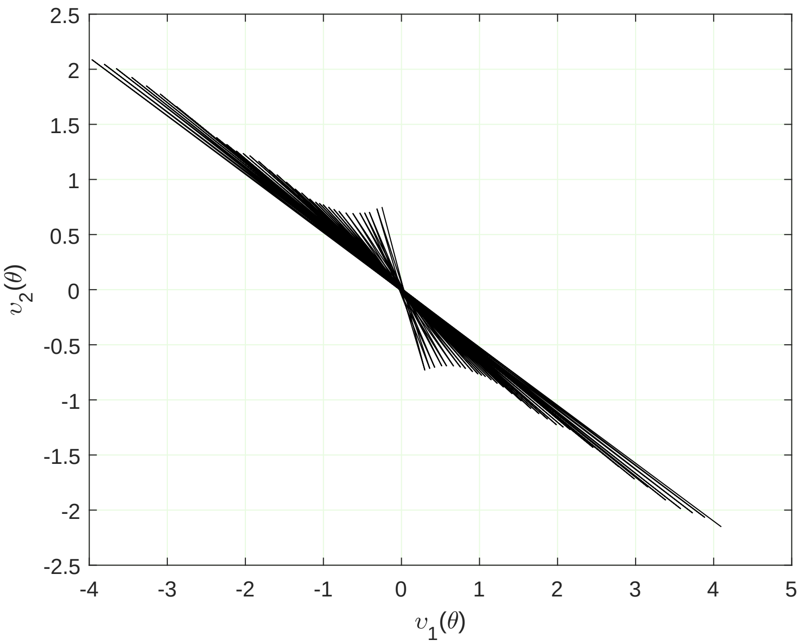

Figure 6: Chaotic behavior of switched un-fixed actuator fault

Basing on Lyapunov theory, we constructed system (44) in the compact form. As the continuous normal actuator is obvious, as shown in the switched case, we calculate the numerical values for known actuators as $R = I$, derivative $\sigma = 0.04$, time-varying bound $d = 0.7$ and uncertain delay $\delta_d = 0.03$. With the help of LMI constraints from Theorem 3, we get the passivity performance index equal $\lambda = 1.0180$. Then, the plausible results can be obtained for the applied controller gain matrices as

$$K = \begin{bmatrix} -2.5371 & -0.1733 \\ -0.2001 & -2.7715 \end{bmatrix}.$$

The state response of the trajectories $\upsilon_1(\theta)$ and $\upsilon_2(\theta)$ are shown in Fig. 7 (g) under passive continuous setting for MNNs under control and in Fig. 7 (h) without control.

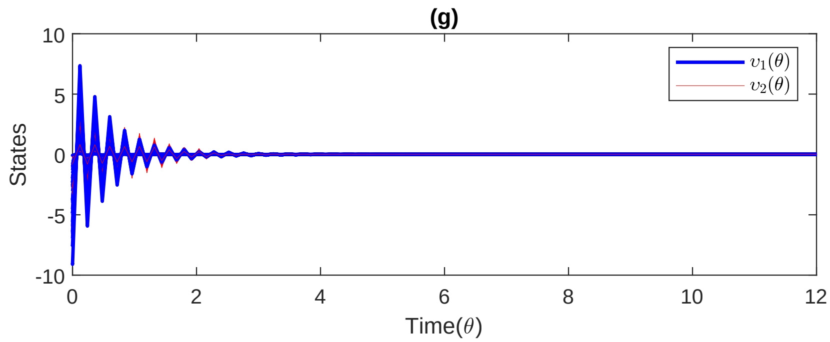

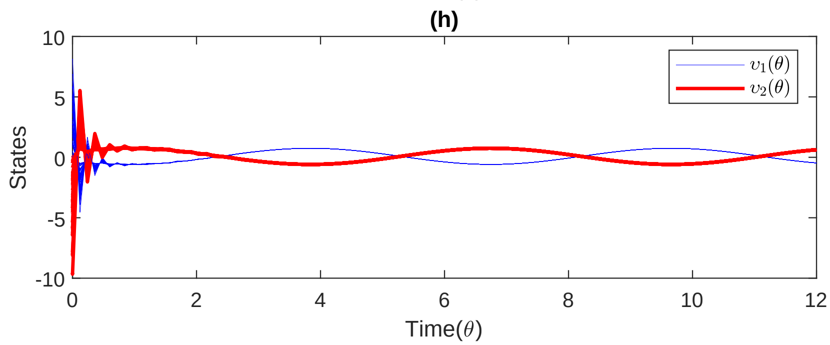

Figure 7: (g) Passive trajectories of continuous normal actuator (44) under reliable controller. (h) Passive trajectories of continuous normal actuator (44) not under reliable controller (representation of actuator fault $R = I$)

(ii) Continuous fixed actuators

Let us design an ideal controller for the proposed system (43), in order to observe the known continuous fixed actuator fault performance in nature

$$\begin{aligned}\begin{bmatrix}\dot{\upsilon}_1(\theta)\\ \dot{\upsilon}_2(\theta)\end{bmatrix} &= \\ &\begin{bmatrix}-0.5 & 0\\ 0 & -0.5\end{bmatrix}\begin{bmatrix}\upsilon_1(\theta)\\ \upsilon_2(\theta)\end{bmatrix} + \begin{bmatrix}-0.1\sin(\upsilon_1(\theta)) & 0.3\cos(\upsilon_1(\theta))\\ 0.2\sin(\upsilon_2(\theta)) & -0.1\cos(\upsilon_2(\theta))\end{bmatrix}\begin{bmatrix}\tilde{g}_1(\upsilon_1(\theta))\\ \tilde{g}_2(\upsilon_2(\theta))\end{bmatrix}\\ &+ \begin{bmatrix}0.2\sin(\upsilon_1(\theta)) & -0.3\cos(\upsilon_1(\theta))\\ -0.5\sin(\upsilon_2(\theta)) & 0.4\cos(\upsilon_2(\theta))\end{bmatrix}\begin{bmatrix}\tilde{g}_1(\upsilon_1(\theta - d(\theta)))\\ \tilde{g}_2(\upsilon_2(\theta - d(\theta)))\end{bmatrix} + RK\begin{bmatrix}\upsilon_1(\theta)\\ \upsilon_2(\theta)\end{bmatrix}.\end{aligned} \tag{45}$$

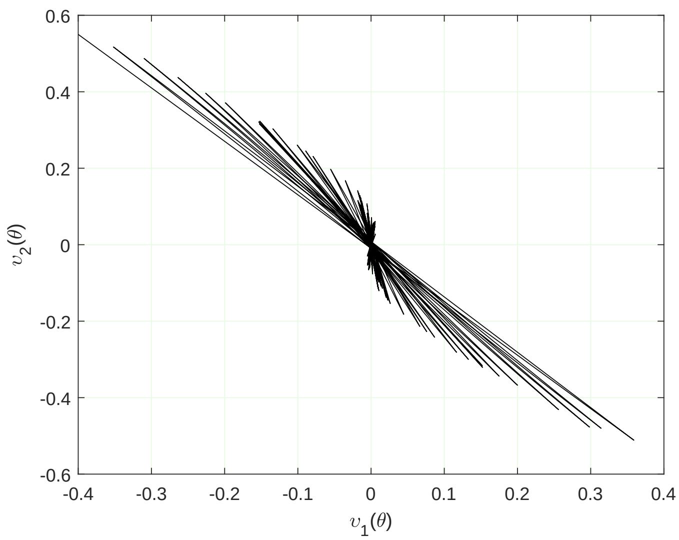

Figure 8: Chaotic behavior of continuous normal actuator fault

By choosing the parameters for continuous fixed actuators with the values of derivative $\sigma = 0.04$, the time-varying bound $d = 0.7$ and uncertain delay $\delta_d = 0.03$, we obtain the actuator, capable of handling the partial shortages. Furthermore, the fixed actuator fault lies in the range of values of $R = diag\{0.67, 0.55\}$. By solving the LMI constraints in Theorem 3, we obtain the passivity performance index equal λ =1.0180, where the feasible solutions are calculated using the MATLAB LMI control toolbox with a reliable state-feedback controller, as follows

$$K = \begin{bmatrix} -3.7867 & -0.2587 \\ -0.3638 & -5.0390 \end{bmatrix}.$$

The graphical simulation for state response of the trajectories $\upsilon_1(\theta)$, $\upsilon_2(\theta)$ is obtained under reliable controller of MNNs for continuous passive system as shown in Fig. 9 (i), while Fig. 9 (j) demonstrates the results, obtained when controller is not applied to the system.

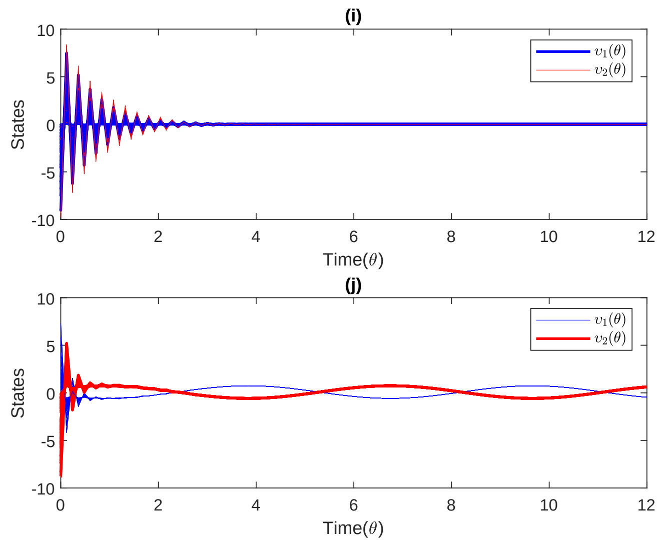

Figure 9: (i) Passive trajectories of continuous fixed actuator (45) under reliable controller. (j) Passive trajectories of continuous fixed actuator (45) not under reliable controller (Representation of actuator fault, when $0 \leq R \leq 1$)

(iii) Continuous un-fixed time-varying actuator

Let us design a controller for the proposed system (43), to observe the unknown continuous un-fixed actuator fault performance in nature

$$\begin{aligned}
\begin{bmatrix} \dot{v}_1(\theta) \\ \dot{v}_2(\theta) \end{bmatrix}
&= \begin{bmatrix} -0.5 & 0 \\ 0 & -0.5 \end{bmatrix} \begin{bmatrix} v_1(\theta) \\ v_2(\theta) \end{bmatrix} + \begin{bmatrix} -0.1\sin(v_1(\theta)) & 0.3\cos(v_1(\theta)) \\ 0.2\sin(v_2(\theta)) & -0.1\cos(v_2(\theta)) \end{bmatrix} \begin{bmatrix} \tilde{g}_1(v_1(\theta)) \\ \tilde{g}_2(v_2(\theta)) \end{bmatrix} \\
&+ \begin{bmatrix} 0.2\sin(v_1(\theta)) & -0.3\cos(v_1(\theta)) \\ -0.5\sin(v_2(\theta)) & 0.4\cos(v_2(\theta)) \end{bmatrix} \begin{bmatrix} \tilde{g}_1(v_1(\theta - d(\theta))) \\ \tilde{g}_2(v_2(\theta - d(\theta))) \end{bmatrix} \\
&+ \Big(\frac{\hat{R} + \check{R}}{2}\Big) K \begin{bmatrix} v_1(\theta) \\ v_2(\theta) \end{bmatrix}. \qquad (46)
\end{aligned}$$

By applying the Schur complement in conjunction with the stabilizing law, we demonstrate that the model achieves effective results in the case of a continuous un-fixed time varying actuator. In order to validate theoretical results via simulation, we select the parameter values as follows: derivative $\sigma = 0.03$,

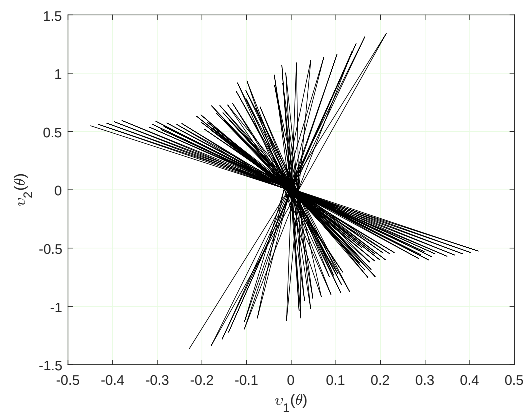

Figure 10: Chaotic behavior of continuous fixed actuator fault

time-varying bound $d = 0.34$ and uncertain delay $\delta_d = 0.04$, corresponding to the un-fixed actuator failure matrix. The actuator faults are assumed to occur within the bounded fault intervals, defined as $0.56 = \underline{r}_1 \leq r_1 \leq \bar{r}_1 = 0.66$ and $0.76 = \underline{r}_2 \leq r_2 \leq \bar{r}_2 = 0.86$, with $R = diag\{0.66, 0.76\}$. A feasible solution is then obtained by solving the LMI constrains, presented in Theorem 4, yielding the passivity performance index value $\lambda = 1.3025$. For these conditions, using the MATLAB LMI control toolbox package with reliable state-feedback controller the gain matrix can be obtained in the following form

$$K = \begin{bmatrix} -2.8850 & -0.1630 \\ -0.1584 & -2.9803 \end{bmatrix}.$$

By fixing the controller to the system (46) as this is shown in Fig. 11 (k), even when an unfixed actuator malfunction occurs, the system can be kept in a stable state, while Fig. 11 (l) presents the trajectories in the unstable case. In general, we found that continuous passive system has a stronger convergence compared to that of switched passive systems.

The chaotic behavior of continuous actuators is also shown in Figs. 8, 10 and 12, respectively. The effects of actuators failures can be noticed in the examined simulation results based on memductance approach. Therefore, we highlight the importance of employing a reliable state-feedback controller in the presence of actuator failures, as it provides an effective way to ensure the internal stability of the considered closed-loop system.

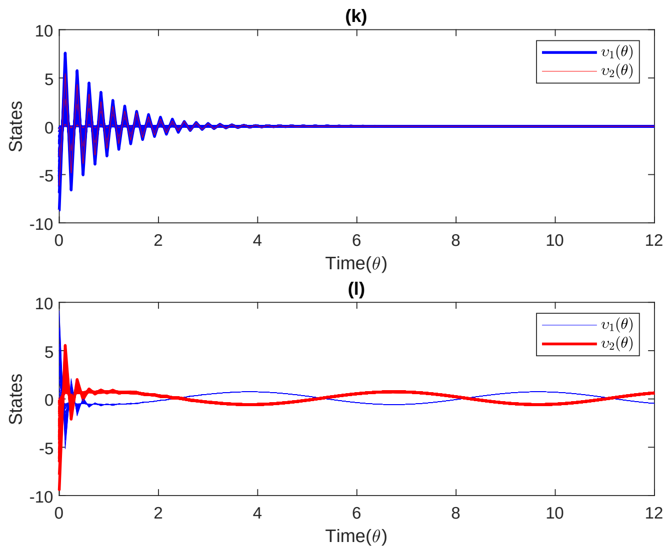

Figure 11: (k) Passive trajectories of continuous un-fixed actuator (46) under reliable controller. (l) Passive trajectories of continuous un-fixed actuator (46) not under reliable controller (representation of actuator fault, when $0 < R < 1$)

Remark 9 *The computational complexity of the proposed model is assumed to be assessed by neglecting the uncertain element, in order to check the variations of performance index for actuators of memductance functions. When the uncertain element δ_d is removed from the time-varying delay for the switched case of LMIs* (10)*, the performance index values for the known case,* (40) *and* (41)*, get increased, while the index values for the unknown case,* (42)*, gets decreased. At the same time, neglecting δ_d in the continuous case of LMI* (29) *makes the performance index increase for known* (44)*,* (45)*, and unknown case* (46)*, which ensures adequate passivity index results.*

5. Conclusion

In this article, we analyzed the problem of reliable passivity for the class of MNNs with uncertain time varying delay. By implementing LMI technique, LKF and congruence transformation we procured the passivity criteria for both state-dependent switched system and state-dependent continuous system by utilizing differential inclusion theory using Lyapunov stability method. Furthermore, we derived some sufficient conditions for known, as well as unknown, actuator fault

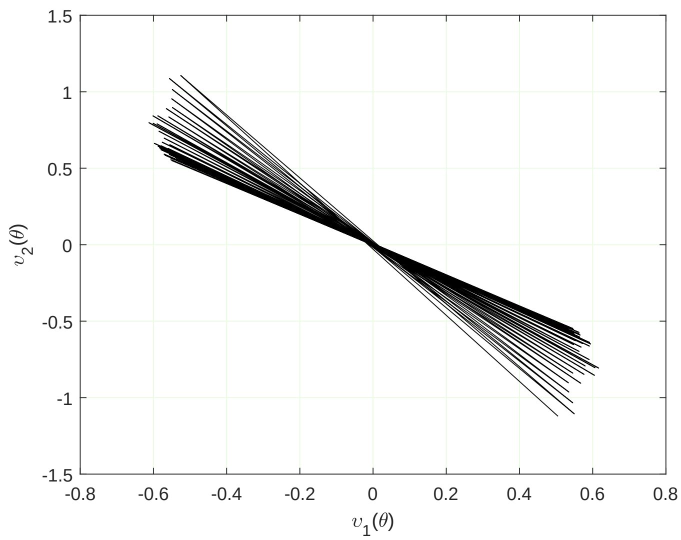

Figure 12: Chaotic behavior of continuous un-fixed actuator fault

matrix using the designed reliable state-feedback controller. Finally, numerical examples are shown for the proposed results to show their validity and effectiveness. On the other hand, future research can be extended to the actuator fault exponential stabilization on memductance function.

Acknowledgement

The first author was supported by University Research Fellowship (PU/AD-3/URF/015723/2020), Periyar University, Salem. The second author's work was funded under FIST programme (SR/FST/MS1-115/2016) by Department of Science and Technology, New Delhi, India.

References

Anbuvithya, R., Mathiyalagan, K., Sakthivel, R. and Prakash, P. (2016) Passivity of memristor-based BAM neural networks with different memductance and uncertain delays. *Cognitive Neurodynamics*, 10, 339-351.

Bevelevich, V. (1968) *Classical Network Synthesis*. Van Nostrand, New York.

Boyd, S., Ghaoui, L. E., Feron, E. and Balakrishnan, V. (1994) *Linear Matrix Inequalities in System and Control Theory*. SIAM, Philadelphia.

Chandrasekar, A., Rakkiyappan, R. and Li, X. (2016) Effects of bounded and unbounded leakage time-varying delays in memristor-based recurrent neural networks with different memductance functions. *Neurocomputing*, 202, 67-83.

Chen, L., Li, T., Chen, Y., Wu, R. and Ge, S. (2019) Robust passivity and feedback passification of a class of uncertain fractional-order linear systems. *International Journal of Systems Science*, 50, 1149-1162.

Chua, L. (1971) Memristor-the missing circuit element. *IEEE Transactions on Circuit Theory*, 18, 507-519.

Ding, Z., Yang, L., Ye, Y., Li, S. and Huang, Z. (2023) Passivity and passification of fractional-order memristive neural networks with time delays. *ISA Transactions*, 137, 314-322.

Ge, C., Park, J. H., Hua, C. and Shi, C. (2019) Robust passivity analysis for uncertain neural networks with discrete and distributed time-varying delays. *Neurocomputing*, 364, 330-337.

Gu, Y., Shen, M., Ren, Y. and Liu, H. (2020) H_∞ finite-time control of unknown uncertain systems with actuator failure. *Applied Mathematics and Computation*, 383, 125375.

Guo, Z., Wang, J. and Yan, Z. (2014) Passivity and passification of memristor based recurrent neural networks with time-varying delays. *IEEE Transactions on Neural Networks and Learning Systems*, 25, 2099-2109.

Huang, Y. L., Qiu, S. H. and Ren, S. Y. (2020) Finite-time synchronization and passivity of coupled memristive neural networks. *International Journal of Control*, 93, 2824-2837.

Junfeng, Z., Li, M. and Raissi, T. (2020) Reliable actuator fault control of positive switched systems with double switchings. *Asian Journal of Control*, 23, 1831-1844.

Li, Y., Zhong, S., Cheng, J., Shi, K. and Ren, J. (2016) New passivity criteria for uncertain neural networks with time-varying delay. *Neurocomputing*, 171, 1003-1012.

Liu, J. and Xu, R. (2016) Passivity analysis of memristive neural networks with mixed time-varying delays and different state-dependent memductance functions. *Advances in Difference Equations*, 245, 1-22.

Padmaja, N. and Balasubramaniam, P. (2022) Results on passivity and design of passive controller for fuzzy neural networks with additive time-varying delays. *Soft Computing*, 26, 9911-9925.

Pershin, Y. V. and Ventra, M. D. (2010) Experimental demonstration of associative memory with memristive neural networks. *Neural Networks*, 23, 881-886.

QIU, S. B., LIU, X. G., WANG, F. X. AND CHEN, Q. (2019) Stability and passivity analysis of discrete-time linear systems with time-varying delay. *Systems and Control Letters*, 134, 104543.

RAJCHAKIT, G. AND SRIRAMAN, R. (2021) Robust passivity and stability analysis of uncertain complex-valued impulsive neural networks with time-varying delays. *Neural Processing Letters*, 53, 581-606.

RAJAVEL, S., SAMIDURAI, R., KILBERT, S.A.J., CAO, J. AND ALSAEDI, A. (2018) Non-fragile mixed H_∞ and passivity control for neural networks with successive time-varying delay components. *Nonlinear Analysis: Modelling and Control*, 23, 159-181.

SAU, N. H., THUAN, M. V. AND HUYEN, N. (2020) Passivity analysis of fractional order neural networks with time-varying delay based on LMI approach. *Circuits, Systems, and Signal Processing*, 39, 5906-5925.

SHAFIYA, M. AND NAGAMANI, G. (2022) New finite-time passivity criteria for delayed fractional-order neural networks based on Lyapunov function approach. *Chaos, Solitons and Fractals*, 158, 112005.

SONG, Q. AND WANG, Z. (2010) New results on passivity analysis of uncertain neural networks with time-varying delays. *International Journal of Computer Mathematics*, 87, 668-678.

SURESH, R. AND MANIVANNAN, A. (2021) Robust stability analysis of delayed stochastic neural networks via Wirtinger based integral inequality. *Neural Computation*, 33, 227-243.

STRUKOV, D. B., SNIDER, G. S., STEWART, D. R. AND WILLIAMS, R. S. (2008) The missing memristor found. *Nature*. 453, 80-83.

SURESH, R., SYED ALI, M. AND SAROHA, S. (2023) Global exponential stability of memristor based uncertain neural networks with time-varying delays via Lagrange sense. *Journal of Experimental and Theoretical Artificial Intelligence*, 35, 275-288.

VADIVEL, R., HAMMACHUKIATTIKUL, P., ZHU, Q. AND GUNASEKARAN, N. (2023) Event-triggered synchronization for stochastic delayed neural networks: Passivity and passification case. *Asian Journal of Control*, 25, 2681-2698.

WANG, L., ZENG, Z., GE, M. F. AND HU, J. (2018) Global stabilization analysis of inertial memristive recurrent neural networks with discrete and distributed delays. *Neural Networks*, 105, 65-74.

WANG, X. B., TANG, H. A., XIA, Q., ZHAO, Q. AND TAN, G. Y. (2022) Feedback control for passivity of memristor based multiple weighted coupled neural networks. *Discrete Dynamics in Nature and Society*, 6920495. https://doi.org/10.1155/2022/6920495

WANG, Y., CAO, Y., GUO, Z. AND WEN, S. (2020) Passivity and passification of memristive recurrent neural networks with multi-proportional delays and impulse. *Applied Mathematics and Computation*, 369, 124838.

Wu, A. and Zeng, Z. (2014) Passivity analysis of memristive neural networks with different memductance functions. *Communications in Nonlinear Science and Numerical Simulation*, 19, 274-285.

Xiao, J. Zhong, S. and Li, Y. (2015) New passivity criteria for memristive uncertain neural networks with leakage and time-varying delays, *ISA Transactions*, 59, 133-148.

Xiao, J. and Zeng, Z. (2020) Finite-time passivity of neural networks with time varying delay. *Journal of the Franklin Institute*, 357, 2437-2456.

Yang, H., Cocquempot, V. and Jiang, B. (2008) Fault tolerance analysis for switched systems via global passivity. *IEEE Transactions on Circuits and Systems II: Express Briefs*, 55, 1279-1283.

Yang, B., Wang, J., Hao, M. and Zeng, H. (2018) Further results on passivity analysis for uncertain neural networks with discrete and distributed delays. *Information Sciences*, 431, 77-86.

Zeng, H. B., Park, J. H. and Shen, H. (2015) Robust passivity analysis of neural networks with discrete and distributed delays. *Neurocomputing*, 149, 1092-1097.

Zhang, G., Hu, J. and Shen, Y. (2015) New results on synchronization control of delayed memristive neural networks. *Non-linear Dynamics*, 81, 1167-1178.

Zhang, J., Li, M. and Raissi, T. (2020) Reliable control for positive switched systems with random nonlinearities. *ISA Transactions*, 108, 48-57.

Zhang, H., Ma, Q., Lu, J., Chu, Y. and Li, Y. (2021) Synchronization control of neutral-type neural networks with sampled-data via adaptive event-triggered communication scheme. *Journal of the Franklin Institute*, 358, 1999-2014.